Supporting Information

Novel multifunctional unimolecular initiators built on natural indole featuring fast photobleaching and visible light/thermal double polymerization

Shang Gong [a], Xiang Wu [a], Qiuyan Liao [a], Shuang Deng [a], Jing Hou [a], Kuangyu Tang [a], Ying Xiong [a], Zhen Li [a], Hongding Tang*[a]

a Engineering Research Center of Organosilicon Compounds & Materials, Ministry of Education, Sauvage Center for Molecular Sciences, College of Chemistry and Molecular Sciences, Wuhan University, Wuhan, 430072, P. R. China.

* Corresponding author: Hongding Tang (E-mail: chhdtang@whu.edu.cn)

Experimental section

Materials

1H-indole-2-carboxaldehyde (ID_2), 1H-indole-3-carboxaldehyde (ID_3), and acryloyl chloride were acquired from Tianjin heowns Snihua Technology Co., Ltd. 1,4-phthalaldehyde, N-methyldiethanolamine (MDEA), and allyl chloride were purchased from Aladdin Industrial Corporation. 1,4-dioxane, potassium hydroxide, cyclopentanone, hydroxylamine hydrochloride, acetyl chloride, sodium acetate (CH_3COONa), ethyl ether, triethylamine (TEA), tetrahydrofuran, ethanol, dichloromethane (DCM), ethyl acetate (EA) and petroleum ether (PE) were obtained from Chinese Pharmaceutical Group Chemical Reagent Co., Ltd. Hexane-1, 6-diyl diacrylate (HDDA, 90%) was obtained from Aladdin. Phenyl-N-tertbutyl-nitrone (PBN) was obtained from TCI. All chemical reagents were used as received without further purification.

Characterization

Molecular determination: ^1H (400 MHz) and ^{13}C (101 MHz) NMR spectra were determined at room temperature on a Bruker-400 spectrometer. Mass spectroscopy was performed by high resolution mass spectrometer (Bruker UltiMate3000 & Compact) in the electrospray ionization (ESI) mode. In addition, Bruker AVANCE NEO 400 MHz NMR spectrometer was used to measure the ^{13}C solid-state NMR spectra of polymers.

Photophysical and photochemical experiments: The UV–vis absorption properties of molecules were characterized using Shimadzu UV-2600 ultraviolet-visible spectrophotometer. The photolysis of IDs in ACN ($[IDs] = 5 \times 10^{-5}$ mol L^{-1}) were carried out under LED@405 nm (50 $mWcm^{-2}$). Fluorescence quantum yields and lifetimes of IDs in ACN ($[IDs] = 5 \times 10^{-5}$ mol L^{-1}) were determined with a FLS980 spectrometer (Edin-burgh Instruments Ltd.), which was equipped with a 450 W xenon lamp.

Theoretical calculations: The theoretical calculations were computed based on Density Function Theory (DFT). The ground state (S_0) geometries were optimized with the Becke three-parameter exchange functional and the Lee Yang Parr correlation functional (B3LYP) using 6-31G basis sets. The excitation energies in the n-th singlet (S_n) and n-th triplet (T_n) states were obtained using the TD-DFT method based on the geometry at ground state (S_0) with B3LYP/6-31G(d). All calculations have been performed using GAUSSIAN 16 package (Revision C.01) [1] and the results were analyzed and visualized with Gauss View 6.0 and Multiwfn [2].

Redox potential measurements: The oxidation and reduction potential of IDs (Eox and Ered) were determined by cyclic voltammetry experiments using a standard three-electrode system with CHI600A (CH, USA) as the electrochemical workstation. Among them, platinum column electrode was the working electrode, platinum wire electrode was the counter electrode and silver electrode was the reference electrode. Ferrocene was applied as the internal standard and the electrolyte was 0.1 mol L^{-1} tetrabutylammonium hexafluorophosphate (Bu_4NPF_6) in ACN solution. ACN solution containing IDs and 0.1 mol L^{-1} Bu_4NPF_6 was prepared, evacuated with argon for 5 min and then measured with a scanning speed of 100 mV s^{-1}.

Detection of the generated CO_2: The generated CO_2 was detected according to the reported method [3]. Four milliliters of ID_3-2 (2×10^{-2} M) ACN solution was added in a transparent sealed glass bottle, which was connected to another glass bottle containing a mixed aqueous solution of Na_2CO_3 (1.8×10^{-4} M) and phenolphthalein (2.1×10^{-4} M). The ID_3-2 solution was irradiated intermittently with 405 nm LED light (100 mW cm^{-2}) for six hours. The Fourier-transform infrared spectroscopy (FT-IR, Nicolet iS10, USA) was used to analyze the chemical structures in the wavenumber range of 500-4000 cm^{-1}.

Electron Paramagnetic Resonance (EPR) experiments: The EPR experiments were conducted using Bruker EMXmicro-6/1. Free radicals were generated under LED@405 nm irradiation at room temperature and captured by phenyl-N-tert-butylnitrone (PBN) in tert-butylbenzene. The concentrations of PBN and IDs were 5×10^{-2} and 8×10^{-3} mol L^{-1}, respectively. The a_N and the a_H represent the hyperfine coupling constants of nitrogen and hydrogen in the PBN radical adduct, respectively.

Photopolymerization experiments: The photopolymerization experiments were carried out on the ThermoNicolet iS10 infrared spectrometer. HDDA was used as the monomer, and the photopolymerization formula was composed of IDs/HDDA in a certain ratio. The formula sandwiched between two KBr pellets was irradiated under a visible LED light source. The LED light source centered at 405 nm was used for initiation of the polymerization, the light intensity was determined using a SRC-1000-TC-QZ-N reference monocrystalline silicon cell system (Oriel, USA), which was calibrated by National Renewable Energy Laboratory of China, A2LA accreditation certificate 2236.01. The double bond conversion was determined from the ratio of the absorbance intensities of C=C (peak at 1634 cm^{-1}) to that o f C=O as the reference (peak at 1717 cm^{-1}) before and after curing with the following formula:[4]

$$\text{Conversion (\%)} = (1 - \frac{A_t}{A_0} \cdot \frac{A_{rb}}{A_{ra}}) \times 100$$

where A_0 and A_t denote the absorbance intensities of C=C before and after curing, while A_{rb} and A_{ra} represent the absorbance intensities of C=O before and after curing, respectively. Each sample was tested three times and errors were kept below 2%.

Curing depth experiments: To explore the applicability of PIs in thick materials, HDDA and PI ID$_3$-2 were selected as the photosensitive components. Firstly, ID$_3$-2/HDDA with different concentrations were injected in cylindrical glassy tubes, which were placed on a plastic shelf. Then, the tubes were irradiated from bottoms for 1 h with LED@405 nm light under Ar atmosphere. Finally, the unpolymerized solutions were rinsed off with ethanol, and the height of the obtained polymer samples were measured.

Thermal stability experiments: Thermogravimetric analysis (TGA, TG209 F1, NETZSCH) was used to explore the thermal stability under nitrogen atmosphere at the heating rates of 10 °C/min ranging from 30 to 600 °C. DSC (DSC3, Mettler-Toledo) was applied to test the melting process of polymer under nitrogen atmosphere at the heating rates of 10 °C/min ranging from 30 to 300 °C.

Synthesis

Synthesis of 1-allyl-1H-indole-2-carbaldehyde (A)

As shown in Scheme 1, allyl indole was prepared according to the literature[5]. A mixture of ID$_2$ (2.90 g, 20.00 mmol), KOH (1.12 g, 20.00 mmol) and 1,4-dioxane (60 mL) was stirred in a round bottom flask (250 mL) at room temperature until complete dissolution. Then, allyl chloride (2.28 g, 30.00 mmol) was slowly dropped into the bottle with a syringe and the reaction mixture was stirred at 80 °C for 10 hours. After, the solvent was stripped off under reduced pressure, and the crude product was dissolved with 30 mL of EA and washed with water (3×50 mL). The organic phase was dried over anhydrous sodium sulfate, filtered, and evaporated under reduced pressure. The raw product was purified by column chromatography (V$_{PE}$: V$_{EA}$=12: 1) to obtain the pale-yellow crystal product (3.11 g, 84%). ^{1}H NMR (400 MHz, CDCl$_3$) δ 9.84 (s, 1H, -C**H**O), 7.71 (d, *J* = 8.1 Hz, 1H, Ar-**H**), 7.40-7.32 (m, 2H, Ar-**H**), 7.24 (s, 1H, -N-C=C**H-**), 7.15 (ddd, *J* = 8.0, 6.3, 1.6 Hz, 1H, Ar-**H**), 5.95 (ddt, *J* = 17.1, 10.3, 5.1 Hz, 1H, -CH$_2$C**H**=CH$_2$), 5.18 (dt, *J* = 5.0, 1.5 Hz, 2H, -C**H**$_2$CH=CH$_2$), 5.07 (dq, *J* = 10.3, 1.2 Hz, 1H, -CH$_2$CH=C**H**$_2$), 4.88 (dq, *J* = 17.1, 1.2 Hz, 1H, -CH$_2$CH=C**H**$_2$). ^{13}C NMR (101 MHz, CDCl$_3$) δ 182.8 (-**C**HO), 140.6 (Ar-**C**), 135.5 (-N**C**=CH-), 133.7 (**C**H=CH$_2$), 127.3 (Ar-**C**), 126.8 (Ar-**C**H), 123.7 (Ar-**C**H), 121.4 (Ar-**C**H), 118.3 (CH=**C**H$_2$), 116.6 (-NC=**C**H-), 111.1 (Ar-**C**H), 47.1 (-**C**H$_2$CH=CH$_2$).

Synthesis of 2-((1-allyl-1H-indol-2-yl) methylene) cyclopentan-1-one (B)

A (2.60 g, 14.00 mmol) and cyclopentanone (2.35 g, 28.00 mmol) were dissolved in ethyl ether (40 mL). Then, 40 mL of KOH (0.78 g, 14.00 mmol) aqueous solution was added and stirred at room temperature for 36 h. After, the crude product was dissolved with 10 mL of EA and washed with water (3×50 mL). Subsequently, the organic phase was dried over anhydrous sodium sulfate, filtered, and evaporated under reduced pressure. Finally, the crude product was purified by column chromatography (V$_{PE}$: V$_{EA}$ = 6: 1) to obtain a yellow solid powder 2.78 g with a yield of 79%. ^{1}H NMR (101 MHz, CDCl$_3$) δ 7.65 (d, *J* = 8.0 Hz, 1H, Ar-**H**), 7.44 (t, *J* = 2.6 Hz, 1H, -C**H**=C**-**), 7.34-7.20 (m, 2H, Ar-**H**), 7.12 (ddd, *J* = 7.8, 5.9, 1.3 Hz, 1H, Ar-H), 6.88 (s, 1H, -N-C=C**H-**, 5.95 (ddt, *J* = 16.3, 10.3, 4.8 Hz, 1H, -CH$_2$C**H**=CH$_2$), 5.12 (d, *J* = 10.4 Hz, 1H, -CH$_2$CH=C**H**$_2$), 4.93-4.78 (m, 3H, -C**H$_2$**CH=C**H**$_2$), 2.97 (td, *J* = 7.3, 2.6 Hz, 2H, -

$CCH_2CH_2C\mathbf{H_2}C{=}O$), 2.45 (t, *J* = 8.0 Hz, 2H, $-CC\mathbf{H_2}CH_2CH_2C{=}O$), 2.17-2.02 (m, 2H, $-CCH_2C\mathbf{H_2}CH_2C{=}O$). ^{13}C NMR (101 MHz, $CDCl_3$) δ 207.7 ($-CH_2\mathbf{C}{=}O$), 138.3 ($-\mathbf{C}CH_2CH_2CH_2C{=}O$), 136.7 (Ar-**C**), 135.1 ($-\mathbf{C}H{=}CH_2$), 133.2 ($-\mathbf{C}H{=}\mathbf{C}-$), 128.2 ($-N-\mathbf{C}{=}CH\mathbf{-}$), 124.2 (Ar-**C**), 121.8 (Ar-**C**H), 120.8 (Ar-**C**H), 119.7 (Ar-**C**H), 117.0 ($-CH{=}\mathbf{C}H_2$), 110.1 (Ar-**C**H), 107.3 ($-N-C{=}\mathbf{CH-}$), 45.6 ($-\mathbf{C}H_2CH{=}CH_2$), 38.8 ($-CCH_2CH_2\mathbf{C}H_2C{=}O$), 30.4 ($-CCH_2\mathbf{C}H_2CH_2C{=}O$), 20.1 ($-C\mathbf{C}H_2CH_2CH_2C{=}O$).

Synthesis of ID_2-Pre

B (2.07 g, 8.25 mmol) and 1,4-phthalaldehyde (1.33 g, 9.90 mmol) were dissolved in anhydrous ethanol (50 mL). Then, KOH (0.46 g, 8.25 mmol) was added and stirred for 15 h at room temperature. A large amount of orange precipitation was observed. Then, the mixture was filtered, and the orange solid was washed with cold ethanol (3×50 mL). After drying in vacuum, the orange solid (2.76 g) was obtained with a yield of 98%. ^1H NMR (400 MHz, $CDCl_3$) δ 10.05 (s, 1H, $-C\mathbf{H}O$), 7.95 (d, *J* = 7.3 Hz, 2H, Ar-**H**), 7.75 (d, *J* = 8.1 Hz, 2H, Ar-**H**), 7.71(s, 1H, $-C\mathbf{H}{=}C\mathbf{-}$)7.69 (d, *J* = 8.0 Hz, 1H, Ar-**H**), 7.59 (s, 1H, $-C{=}C\mathbf{H-}$), 7.38-7.27 (m, 2H, Ar-**H**), 7.15 (t, *J* = 7.2 Hz 1H, Ar-**H**), 6.97 (s, 1H, $-N-C{=}C\mathbf{H-}$), 5.99 (ddt, *J* = 17.0, 10.4, 4.6 Hz, 1H, $-CH_2C\mathbf{H}{=}CH_2$), 5.16 (d, *J* = 10.3 Hz, 1H, $-CH_2CH{=}C\mathbf{H_2}$), 5.00-4.85 (m, 3H, $-C\mathbf{H_2}CH{=}C\mathbf{H_2}$), 3.25-3.16 (m, 2H, $-C\mathbf{H_2}CH_2-$), 3.16-3.06 (m, 2H, $-CH_2C\mathbf{H_2}-$). ^{13}C NMR (101 MHz, $CDCl_3$) δ 195.4 ($-\mathbf{C}{=}O$), 191.9 ($-\mathbf{C}HO$), 142.1 ($O{=}C-\mathbf{C}{=}CH-$), 141.4 ($O{=}C-\mathbf{C}{=}CH-$), 138.7 (Ar-**C**), 137.4 (Ar-**C**), 136.4 (Ar-**C**), 135.3 ($O{=}C-C{=}\mathbf{C}H-$), 133.2 ($-CH_2\mathbf{CH}{=}CH_2$), 131.9 ($O{=}C-C{=}\mathbf{C}H-$), 131.3 (Ar-**C**H), 130.30 (Ar-**C**H), 128.3 ($-N-\mathbf{C}{=}CH-$), 124.8 (Ar-**C**), 122.1 (Ar-**C**H), 122.0 (Ar-**C**H), 121.0 (Ar-**C**H), 117.2 ($-CH_2CH{=}\mathbf{C}H_2$), 110.3 (Ar-**C**H), 108.4 ($-N-C{=}\mathbf{C}H-$), 45.6 ($-\mathbf{C}H_2CH{=}CH_2$), 27.5 ($-\mathbf{C}H_2CH_2-$), 26.8 ($-\mathbf{C}H_2CH_2-$). HR-MS (ESI) m/z: calcd for $C_{25}H_{22}NO_2$ $[M+H]^+$, 368.164635; found, 368.164505.

Synthesis of ID_2-OH

A mixture of ID_2-Pre (0.37 g, 1.00 mmol), hydroxylamine hydrochloride (0.35 g, 5.00 mmol), and CH_3COONa (0.16 g, 2.00 mmol) was dissolved and stirred in anhydrous ethanol (50 mL) for 3 h at room temperature. After, the solvent was stripped off under reduced pressure, and the crude product was dissolved with 30 mL of DCM and washed with water (3×50 mL). Then, the organic phase was dried over anhydrous sodium sulfate, filtered, and evaporated under reduced pressure to obtain an orange red product (0.25 g, 72%). ^{1}H NMR (400 MHz, DMSO-d_6) δ 11.52 (s, 1H, -N-O**H**), 8.23 (s, 1H, -C**H**=N-), 7.92-7.66 (m, 5H, Ar-**H**), 7.56 (d, *J* = 12.8 Hz, 2H, -C**H**=C, Ar-**H**), 7.46 (s, 1H, -C=C**H-**), 7.29 (t, *J* = 7.0 Hz, 1H, Ar-**H**), 7.14 (t, *J* = 6.9 Hz, 1H, Ar-**H**), 7.08 (s, 1H, -N-C=C**H-**), 6.13-6.00 (m, 1H, -CH$_2$C**H**=CH$_2$), 5.11 (m, 3H, -C**H**$_\mathbf{2}$CH=C**H**$_2$), 4.72 (d, *J* = 17.0 Hz, 1H, -CH$_2$CH=C**H**$_2$), 3.19 (s, 2H, -C**H**$_2$CH$_2$-), 3.10 (s, 2H, -CH$_2$C**H**$_2$-).^{13}C NMR (101 MHz, DMSO-d_6) δ 194.3 (**C**=O), 147.8 (N=**C**H-), 139.0 (O=C-**C**=CH-), 138.0 (O=C-**C**=CH-), 137.9 (Ar-**C**), 136.2 (O=C-C=**C**H-), 134.8 (Ar-**C**), 134.4 (Ar-**C**), 133.9 (O=C-C=**C**H-), 131.6 (-CH$_2$**C**H=CH$_2$), 131.1 (Ar-**C**H), 129.7 (Ar-**C**H), 127.5 (Ar-**C**H), 126.8 (-N-**C**=CH-), 124.0 (Ar-**C**), 121.5 (Ar-**C**H), 120.4 (Ar-**C**H), 120.11 (Ar-**C**H), 115.7 (-CH$_2$CH=**C**H$_2$), 110.4 (Ar-**C**H), 107.3 (-N-C=**C**H-), 44.7 (-**C**H$_2$CH=CH$_2$), 28.7 (-**C**H$_2$CH$_2$-), 28.6 (-CH$_2$**C**H$_2$-). HR-MS (ESI) m/z: calcd for $C_{25}H_{23}N_2O_2$ [M+H]$^+$, 383.175422; found, 383.175404.

Synthesis of ID$_2$-1

ID$_2$-OH (0.75 g, 1.95 mmol) and TEA (0.59 g, 5.85 mmol) were dissolved in tetrahydrofuran (30 mL). Then, the mixture was cooled to 0 °C and kept stirring for 1 h. Then, 5 mL of acryloyl chloride (0.36 g, 3.90 mmol) tetrahydrofuran solution was added dropwise, and the mixture was stirred for 5 h. The solvent was evaporated under reduced pressure, and the crude product was extracted with EA (3 × 50 mL). Then, the organic phase was dried over anhydrous sodium sulfate, filtered, and evaporated under reduced pressure. The crude product was purified by column chromatography (V_{PE}: V_{EA}: V_{DCM}=6: 1: 8) to obtain orange solid powder 0.37 g with a yield of 44%. ^{1}H NMR (400 MHz, $CDCl_3$) δ 8.42 (s, 1H, -C**H**=N-), 7.82 (d, *J* = 8.1 Hz, 2H, Ar-**H**), 7.68 (d, *J* = 7.6 Hz, 2H, Ar-**H**), 7.64 (d, *J* = 8.2 Hz, 2H, Ar-**H**), 7.55 (s, 1H, -C**H**=C-), 7.30 (t, *J* = 8.5 Hz, 1H, Ar-**H**), 7.29 (s, 1H, -C=C**H-**), 7.14 (t, *J* = 7.5 Hz, 1H, Ar-**H**), 6.95 (s, 1H, -N-C=C**H-**), 6.61 (d, *J* = 17.3 Hz, 1H, -COCH=C**H**$_2$), 6.27 (dd, *J* = 17.3, 10.5 Hz, 1H, -COC**H**=CH$_2$), 5.98 (d, *J* = 10.6 Hz, 1H, -COCH=C**H**$_2$), 5.98 (ddt, *J* = 16.8, 10.4, 4.6 Hz 1H, -CH$_2$C**H**=CH$_2$), 5.15 (d, *J* = 10.4 Hz, 1H, -CH$_2$CH=C**H**$_2$), 4.89 (d, *J* = 16.8, 4.6

Hz, 3H, -C**H**$_2$CH=C**H**$_2$), 3.15 (t, *J* = 3.6 Hz, 2H, -C**H**$_2$CH$_2$-), 3.08 (t, *J* = 3.8 Hz, 2H, -CH$_2$C**H**$_2$-).^{13}C NMR (101 MHz, CDCl$_3$) δ 195.2 (=CH**C**OCH=), 163.7 (-**C**OCH=CH$_2$), 155.9 (N=**C**H-), 140.0 (O=C-**C**=CH-), 139.3 (O=C-**C**=CH-), 138.4 (Ar-**C**), 137.5 (Ar-**C**), 135.2 (-COCH=**C**H$_2$), 133.0 (-CH$_2$**C**H=CH$_2$), 132.7(O=C-C=**C**H-), 132.1(O=C-C=**C**H-), 131.1 (Ar-**C**), 130.6 (Ar-**C**H), 128.9 (Ar-**C**H), 128.1 (-CO**C**H=CH$_2$), 126.2 (-N-**C**=CH-), 124.4 (Ar-**C**), 121.8 (Ar-**C**H), 121.4 (Ar-**C**H), 120.8 (Ar-**C**H), 116.9 (-CH$_2$CH=**C**H$_2$), 110.0 (Ar-**C**H), 108.0 (-N-C=**C**H-), 45.4 (-**C**H$_2$CH=CH$_2$), 27.3 (-**C**H$_2$CH$_2$-), 26.5 (-CH$_2$**C**H$_2$-). HR-MS (ESI) m/z: calcd for $C_{28}H_{25}N_2O_3$ $[M+H]^+$, 437.188076; found, 437.185969.

Synthesis of ID$_2$-2

ID$_2$-OH (0.38 g, 1.00 mmol) and TEA (0.30 g, 3.00 mmol) were dissolved in tetrahydrofuran (30 mL). Then, the mixture was cooled to 0 °C and kept stirring for 1 h. After, 5 mL of acetyl chloride (0.16 g, 2.00 mmol) tetrahydrofuran solution was added dropwise and stirred for 5 h. The solvent was evaporated under reduced pressure, and the crude product was extracted with EA (3 × 50 mL). Then, the organic phase was dried over anhydrous sodium sulfate, filtered, and evaporated under reduced pressure. The crude product was purified by column chromatography (V_{PE}: V_{EA}: V_{DCM}=4: 1: 3) to obtain orange solid powder 0.19 g with a yield of 48%. ^{1}H NMR (400 MHz, CDCl$_3$) δ 8.36 (s, 1H, -C**H**=N-), 7.79 (d, *J* = 8.0 Hz, 2H, Ar-**H**), 7.68 (d, *J* = 7.2 Hz, 2H, Ar-**H**), 7.63 (d, *J* = 8.2 Hz, 2H, Ar-**H**), 7.54 (s, 1H, -C**H**=C-), 7.63 (s, 1H, -C=C**H-**), 7.29 (t, *J* = 8.2 Hz, 1H, Ar-**H**), 7.14 (t, *J* = 7.6 Hz, 1H, Ar-**H**), 6.94 (s, 1H, -N-C=C**H-**), 5.97 (ddt, *J* = 16.4, 10.4, 4.5 Hz, 1H, -CH$_2$C**H**=CH$_2$), 5.14 (d, *J* = 10.4 Hz, 1H, CH$_2$CH=C**H**$_2$), 4.89 (d, *J* = 16.4, 4.5 Hz, 3H, -C**H**$_2$CH=C**H**$_2$), 3.14 (t, *J* = 3.5 Hz, 2H, -C**H**$_2$CH$_2$-), 3.08 (t, *J* = 3.5 Hz, 2H, -CH$_2$C**H**$_2$-), 2.24 (s, 3H,-CH$_3$). ^{13}C NMR (101 MHz, CDCl$_3$) δ 195.2 (=CH**C**OCH=), 168.7 (CH$_3$**C**O-), 155.3 (N=**C**H-), 140.0 (O=C-**C**=CH-), 139.3 (O=C-**C**=CH-), 138.4 (Ar-**C**), 137.4 (Ar-**C**), 135.1 (O=C-C=**C**H-), 133.0 (-CH$_2$**C**H=CH$_2$), 132.1 (O=C-C=**C**H-), 131.1 (Ar-**C**), 130.6 (Ar-**C**H), 128.8 (Ar-**C**H), 128.1 (-N-**C**=CH-), 124.4 (Ar-**C**), 121.8 (Ar-**C**H), 121.4 (Ar-**C**H), 120.8 (Ar-**C**H), 116.9 (-CH$_2$CH=**C**H$_2$), 110.0 (Ar-**C**H), 108.0 (-N-C=**C**H-), 45.4 (-**C**H$_2$CH=CH$_2$), 27.3 (-

$\mathbf{C}H_2CH_2$-), 26.5 (-$CH_2\mathbf{C}H_2$-), 19.7 ($\mathbf{C}H_3CO$-). HR-MS (ESI) m/z: calcd for $C_{27}H_{25}N_2O_3$ $[M+H]^+$, 425.186111; found, 425.185969.

Synthesis of 1-allyl-1H-indole-3-carbaldehyde (C)

A similar synthetic method as that described for A was used to prepare C, and a black product was obtained. The raw product was purified by column chromatography (V_{PE}: V_{EA}=2: 1) to obtain the pale-yellow crystal with a yield of 73%. ^1H NMR (400 MHz, $CDCl_3$) δ 10.00 (s, 1H, -$C\mathbf{H}O$), 8.31 (dd, *J* = 8.0, 4.1 Hz, 1H, Ar-**H**), 7.72 (s, 1H, N-$C\mathbf{H}$=C-), 7.43-7.28 (m, 3H, Ar-**H**), 6.02 (ddt, *J* = 17.1, 10.6, 5.5 Hz, 1H, -$CH_2C\mathbf{H}$=CH_2), 5.32 (d, *J* = 10.3 Hz, 1H, -CH_2CH=$C\mathbf{H}_2$), 5.19 (d, *J* = 17.0 Hz, 1H, -CH_2CH=$C\mathbf{H}_2$), 4.78 (d, *J* = 5.5 Hz, 2H, -$C\mathbf{H}_2CH$=CH_2). ^{13}C NMR (101 MHz, $CDCl_3$) δ 184.7 (-**C**HO), 138.4 (Ar-**C**), 137.4 (N-**C**H=C-), 131.8 (-$CH_2\mathbf{C}H$=CH_2), 125.5 (Ar-**C**), 124.2 (Ar-**C**H), 123.1 (Ar-**C**H), 122.2 (Ar-**C**H), 119.2 (-**C**-CHO), 118.5 (-CH_2CH=$\mathbf{C}H_2$), 110.4 (Ar-**C**H), 49.6 (-$\mathbf{C}H_2CH$=CH_2).

Synthesis of 2-((1-allyl-1H-indol-3-yl) methylene) cyclopentan-1-one (D)

C (2.24 g, 12.10 mmol) and cyclopentanone (3.05 g, 36.30 mmol) were dissolved in anhydrous ethanol (50 mL) under N_2 atmosphere. Then, pyrrolidine (0.24 g, 3.41 mmol) was slowly dropped into the bottle with a syringe and stirred for 10 min. After, the temperature was gradually raised to 50 °C for 2 hours. Then, the solvent was evaporated under reduced pressure, and the crude product was extracted with EA (3 × 50 mL). After, the organic phase was dried over anhydrous sodium sulfate, filtered, and evaporated under reduced pressure. The crude product was purified by column chromatography (V_{PE}: V_{EA} = 6: 1) to obtain a yellow solid powder 1.08 g with a yield of 36%. ^1H NMR (400 MHz, $CDCl_3$) δ 7.87 (d, *J* = 7.5 Hz, 1H, Ar-**H**), 7.81 (t, *J* = 2.2 Hz, 1H, -C=C**H-**), 7.37 (s, 1H, -N-C**H**=C**-**), 7.33 (d, *J* = 7.96 Hz, 1H, Ar-**H**), 7.87 (d, *J* = 6.80 Hz, 1H, Ar-**H**), 7.25-7.17(m, 3H, Ar-**H**), 6.00 (ddt, *J* = 17.0, 10.5, 5.4 Hz, 1H, -$CH_2C\mathbf{H}$=CH_2), 5.26 (d, *J* = 10.2 Hz, 1H, -CH_2CH=$C\mathbf{H}_2$), 5.13 (d, *J* = 17.1 Hz, 1H, -CH_2CH=$C\mathbf{H}_2$), 4.77 (d, *J* = 5.4 Hz, 2H, -$C\mathbf{H}_2CH$=CH_2), 2.82 (td, *J* = 7.3, 2.3 Hz, 2H, -C-CH_2-CH_2-$C\mathbf{H}_2$-C=O), 2.42 (t, *J* = 7.9 Hz, 2H, -C-$C\mathbf{H}_2$-CH_2-CH_2-C=O), 2.15-2.00 (m, 2H, -C-CH_2-$C\mathbf{H}_2$-CH_2-C=O). ^{13}C NMR (101 MHz, $CDCl_3$) δ 207.6 (**C**=O), 136.3 (-

CH=**C**-), 132.5 (Ar-**C**), 131.0 (-**C**H=C-), 129.9 (-N-**C**H=C**-**), 128.8 (-CH$_2$**C**H=CH$_2$), 123.8 (Ar-**C**), 123.2 (Ar-**C**H), 121.1 (Ar-**C**H), 119.3 (Ar-**C**H), 118.3 (-CH$_2$CH=**C**H$_2$), 112.9 (-N-CH=**C-**), 110.2 (Ar-**C**H), 49.4 (-**C**H$_2$CH=CH$_2$), 38.2 (-CCH$_2$CH$_2$**C**H$_2$C=O), 30.3 (-C**C**H$_2$CH$_2$CH$_2$C=O), 19.9 (-CCH$_2$CH$_2$**C**H$_2$C=O).

Synthesis of ID$_3$-Pre

A similar synthetic method as that described for ID$_2$-Pre was used to prepare ID$_3$-Pre, and obtained orange powder with a yield of 93%. ^{1}H NMR (400 MHz, DMSO-d_6) δ 10.08 (s, 1H, -C**H**O), 8.03 (d, J = 8.2 Hz, 2H, Ar-**H**), 7.99 (s, 1H, -N-C**H**=C), 7.96 (d, J = 7.7 Hz, 1H, Ar-**H**), 7.93 (d, J = 8.4 Hz, 2H, Ar-**H)**, 7.92 (s, 1H, -C**H**=C**-**), 7.58 (d, J = 8.0 Hz, 1H, Ar-**H**), 7.46 (t, J = 2.6 Hz,1H, -C=C**H-**), 7.32 (t, J = 7.6 Hz, 1H, Ar-**H**), 7.27 (t, J = 7.4 Hz, 1H, Ar-**H**), 6.10 (ddt, J = 17.1, 10.3, 5.5 Hz, 1H, -CH$_2$C**H**=CH$_2$), 5.25 (dq, J = 10.2, 1.3 Hz, 1H , -CH$_2$CH=C**H$_2$**), 5.16 (dq, J = 17.1, 1.4 Hz, 1H, -CH$_2$CH=C**H$_2$**), 5.02 (d, J = 5.4 Hz, 2H, -C**H$_2$**CH=CH$_2$), 3.22 (t, J = 4.1 Hz, 2H, -C**H**$_2$CH$_2$-), 2.99 (t, J = 4.1 Hz, 2H, -CH$_2$C**H**$_2$-). ^{13}C NMR (101 MHz, DMSO-d_6) δ 193.7 (**C**=O), 192.7 (-**C**HO), 142.5 (-CH=**C**-), 141.5 (-**C**H=C-), 136.0 (-**C**=CH-), 135.6 (Ar-**C**), 133.7 (Ar-**C**), 132.3 (-N-**C**H=C-), 131.9 (-C=**C**H-), 130.8 (Ar-**C**), 129.8 (Ar-**C**H), 129.1 (-CH$_2$**C**H=CH$_2$), 128.1 (Ar-**C**), 125.0 (Ar-**C**H), 122.9 (Ar-**C**H), 121.1 (Ar-**C**H), 118.6 (-CH$_2$CH=**C**H$_2$), 117.5 (-N-CH=**C**-), 111.9 (Ar-**C**H), 111.0 (-**C**H$_2$CH=CH$_2$), 48.7 (-**C**H$_2$CH$_2$-), 26.8 (-CH$_2$**C**H$_2$-). HR-MS (ESI) m/z: calcd for $C_{25}H_{22}NO_2$ $[M+H]^+$, 368.164384; found, 368.164505.

Synthesis of ID$_3$-OH

A similar synthetic method as that described for ID$_2$-OH was used to prepare ID$_3$-OH, and obtained orange powder with a yield of 91%. ^{1}H NMR (400 MHz, DMSO-d_6) δ 11.46 (s, 1H, -N-O**H**), 8.23 (s, 1H, -C**H**=N-), 7.98 (s, 1H, -N-C**H**=C-), 7.95 (d, J = 7.6 Hz, 1H, Ar-**H**), 7.89 (s, 1H, -C**H**=C**-**), 7.75 (dd, J = 10.3, 9.0 Hz, 4H, Ar-**H**), 7.58 (d, J = 8.0 Hz, 1H, Ar-**H**), 7.41 (s, 1H, -C=C**H-**), 7.32 (t, J = 7.3 Hz, 1H, Ar-**H**), 7.26 (t, J =7.6 Hz, 1H, Ar-**H**), 6.10 (ddt, J = 16.9, 10.3, 5.5 Hz, 1H, -CH$_2$C**H**=CH$_2$), 5.25 (d, J = 10.2 Hz, 1H, -CH$_2$CH=C**H**$_2$), 5.16 (d, J = 17.1 Hz, 1H, -CH$_2$CH=C**H**$_2$), 5.03 (d, J = 4.9 Hz, 2H, -C**H**$_2$CH=CH$_2$), 3.19 (t, J = 4.1 Hz, 2H, -C**H**$_2$CH$_2$-), 2.99 (t, J = 3.9

Hz, 2H, -CH_2**C**H_2-). ^{13}C NMR (101MHz, DMSO-*d$_6$*) 193.8 (**C**=O), 147.8 (-CH=**C**-), 140.0 (-**C**H=N-), 136.5 (-**C**H=C-), 136.0 (-**C**=CH-), 133.7 (Ar-**C**), 133.5 (Ar-**C**), 132.2 (-N-**C**H=C-), 132.1(-C=**C**H-), 130.8 (Ar-**C**), 130.1 (Ar-**C**H), 128.1 (-CH_2**C**H=CH_2), 126.8 (Ar-**C**H), 124.4 (Ar-**C**), 122.8 (Ar-**C**H), 121.0(Ar-**C**H), 118.6(Ar-**C**H), 117.5 (-CH_2CH=**C**H_2), 111.9(-N-CH=**C**-), 111.0 (Ar-**C**H), 48.7(-**C**H_2CH=**C**H_2), 26.9 (-**C**$H_2$$CH_2$-), 25.8 (-$CH_2$**C**$H_2$-). HR-MS (ESI) m/z: calcd for $C_{25}H_{23}NO_2$ $[M+H]^+$, 383.175177; found, 383.175404.

Synthesis of ID$_3$-1

A similar synthetic method as that described for ID$_2$-1 was used to prepare ID$_3$-1, and a black product was obtained. The raw product was purified by column chromatography (V_{PE}: V_{DCM}: V_{EA} =5: 3: 1) to give orange powder with a yield of 58%. ^{1}H NMR (400 MHz, $CDCl_3$) δ 8.40 (s, 1H, -C**H**=N-), 8.06 (s, 1H, -C**H**=C-), 7.94 (d, *J* = 6.4 Hz, 1H, Ar-**H**), 7.79 (d, *J* = 8.1 Hz, 2H, Ar-**H**), 7.61 (d, *J* = 8.1 Hz, 2H, Ar-**H**), 7.50 (s, 1H, -C=C**H-**), 7.41 (s, 1H, -N-C**H**=C-), 7.37-7.26 (m, 3H, Ar-**H**), 6.60 (d, *J* = 17.3 Hz, 1H, -COCH=C**H**$_2$), 6.26 (dd, *J* = 17.3, 10.5 Hz, 1H, -COC**H**=CH_2), 6.04 (ddt, *J* = 17.0, 10.4, 5.3 Hz 1H, -CH_2C**H**=CH_2), 5.98 (d, *J* = 10.9 Hz, 1H, -COCH=C**H**$_2$), 5.29 (d, *J* = 10.2 Hz, 1H, -CH_2CH=C**H**$_2$), 5.17 (d, *J* = 17.0 Hz, 1H, -CH_2CH=C**H**$_2$), 4.79 (d, *J* = 5.0 Hz, 2H, -C**H**$_2$CH=CH_2), 3.12 (t, *J* = 4.4 Hz, 2H, -C**H**$_2$$CH_2$-), 2.88 (t, *J* = 4.6 Hz, 2H, -CH_2C**H**$_2$-). ^{13}C NMR (101 MHz, $CDCl_3$) δ 195.1 (**C**=O), 163.7 (N-O-**C**=O), 156.0 (-**C**H=N-), 140.9 (-CH=**C**-), 139.7 (-**C**H=C-), 136.4 (-**C**=CH-), 132.7 (Ar-C), 132.4 (Ar-C), 132.2 (-N-**C**H=C-), 130.9 (**C**H_2=CH-), 130.8 (-C=**C**H-), 130.6 (CH_2=**C**H-), 130.2 (-CH_2**C**H=CH_2), 128.8 (Ar-**C**), 126.3 (Ar-**C**H), 126.1 (Ar-**C**H), 123.4 (Ar-**C**), 121.4 (Ar-**C**H), 119.5 (Ar-**C**H), 118.5 (-CH_2CH=**C**H_2), 113.6 (-N-CH=**C**-), 110.3 (Ar-**C**H), 49.6 (-**C**H_2CH=CH_2), 27.4 (-**C**$H_2$$CH_2$-), 26.5 (-$CH_2$**C**$H_2$-). HR-MS (ESI) m/z: calcd for $C_{28}H_{25}N_2O_3$ $[M+H]^+$, 437.188043; found, 437.185969.

Synthesis of ID$_3$-2

A similar synthetic method as that described for ID$_2$-2 was used to prepare ID$_3$-2, and a black product was obtained. The raw product was purified by column chromatography (V_{PE}: V_{DCM}: V_{EA} = 6: 3: 1) to give orange powder with a yield of 60%.

^{1}H NMR (400 MHz, $CDCl_3$) δ 8.35 (s, 1H, -C**H**=N-), 8.08 (s, 1H, -C**H**=C-), 7.95 (d, *J* = 6.7 Hz, 1H, Ar-**H**), 7.78 (d, *J* = 8.1 Hz, 2H, Ar-**H**), 7.62 (d, *J* = 8.0 Hz, 2H, Ar-**H**), 7.51 (s, 1H, -C=C**H-**), 7.43 (s, 1H, -N-C**H**=C-), 7.38-7.26(m, 3H, Ar-**H**), 6.03 (ddt, *J* = 17.0 10.4, 5.4Hz, 1H, -CH_2C**H**=CH_2), 5.29 (d, *J* = 10.2 Hz, 1H, -CH_2CH=C**H**$_2$), 5.17 (d, *J* = 17.1 Hz, 1H, -CH_2CH=C**H**$_2$), 4.80 (d, *J* = 5.2 Hz, 2H, -C**H**$_2$CH=CH_2), 3.12 (t, *J* = 4.2 Hz, 2H, C**H**$_2$$CH_2$-), 2.93 (t, *J* = 4.7 Hz, 2H, CH_2C**H**$_2$-), 2.24 (s, 3H,-COC**H**$_3$). ^{13}C NMR (101 MHz, $CDCl_3$) δ 195.1 (**C**=O), 168.8 (CH_3**C**O-), 155.4 (**C**H=N-), 140.9 (-CH=**C**-), 139.7 (-CH=C-), 136.4 (-**C**=CH-), 132.4 (Ar-**C**), 132.2 (Ar-**C**), 130.9 (-CH_2**C**H=CH_2), 130.8 (-N-**C**H=C-), 130.6 (-C=**C**H-), 130.2 (Ar-**C**), 128.7 (Ar-**C**H), 126.2 (Ar-**C**H), 123.4 (Ar-**C**), 121.5 (Ar-**C**H), 119.5 (Ar-**C**H), 118.5 (-CH_2CH=**C**H$_2$), 113.6 (-N-CH=**C**-), 110.3 (Ar-**C**H), 49.6 (-**C**H$_2$CH=CH_2), 27.5 (-**C**H$_2$$CH_2$-), 26.5 (-$CH_2$**C**H$_2$-), 19.7 (**C**H$_3$CO-). HR-MS (ESI) m/z: calcd for $C_{27}H_{25}N_2O_3$ $[M+H]^+$, 425.186537; found, 425.185969.

Table S1. Absorption properties of IDs derivatives in ACN and TD-DFT data relative to their three lowest energy electronic transitions.

PIs	**Experimental**	**Theoretical**			
	λ_{abs} (ε_{abs}) [nm (10^4 M^{-1} cm^{-1})]	λ_{abs}(nm)	*f*	ΔE S_0-S_1(eV) ΔE S_0-S_2(eV)	Main transitions (fraction, type)
ID_2-Pre	430 (2.34)	492 ^{a}	0.7047 ^{a}	2.52 ^{a}	H→L (0.99, π–π*) ^{a}
		432 ^{b}	0.3969 ^{b}	2.87 ^{b}	H_{-1}→L (0.98, π–π*) ^{b}
ID_2-OH	425 (2.79)	472 ^{a}	1.0402 ^{a}	2.63 ^{a}	H→L (0.99, π–π*) ^{a}
		419 ^{b}	0.5239 ^{b}	2.96 ^{b}	H_{-1}→L (0.92, π–π*) ^{b}
ID_2-1	426 (2.61)	486 ^{a}	0.9032 ^{a}	2.55 ^{a}	H→L (0.99, π–π*) ^{a}
		427 ^{b}	0.5022 ^{b}	2.90 ^{b}	H_{-1}→L (0.98, π–π*) ^{b}
ID_2-2	425 (2.55)	482 ^{a}	0.8937 ^{a}	2.57 ^{a}	H→L (0.99, π–π*) ^{a}
		425 ^{b}	0.4954 ^{b}	2.92 ^{b}	H_{-3}→L (0.98, π–π*) ^{b}

Table S2 Group contribution to $S_0 \rightarrow S_1$ transition of oxime esters.

Groups		1	2	3	4	5
ID_3-Pre	Hole	12.151	74.058	5.809	4.872	0.316
	Electron	1.449	14.801	17.251	48.553	16.252
	Overlap	4.197	33.108	10.01	15.381	2.266
ID_3-OH	Hole	11.921	72.594	4.732	6.944	0.995
	Electron	1.847	19.790	21.678	45.426	9.437
	Overlap	4.693	37.903	10.128	17.760	3.064
ID_3-1	Hole	12.066	73.368	5.188	5.915	0.661
	Electron	1.460	15.230	17.578	45.182	18.912
	Overlap	4.197	33.427	9.550	16.348	3.536
ID_3-2	Hole	12.083	73.624	5.445	5.493	0.522
	Electron	1.569	16.281	18.633	47.435	13.723
	Overlap	4.354	34.621	10.073	16.141	2.676

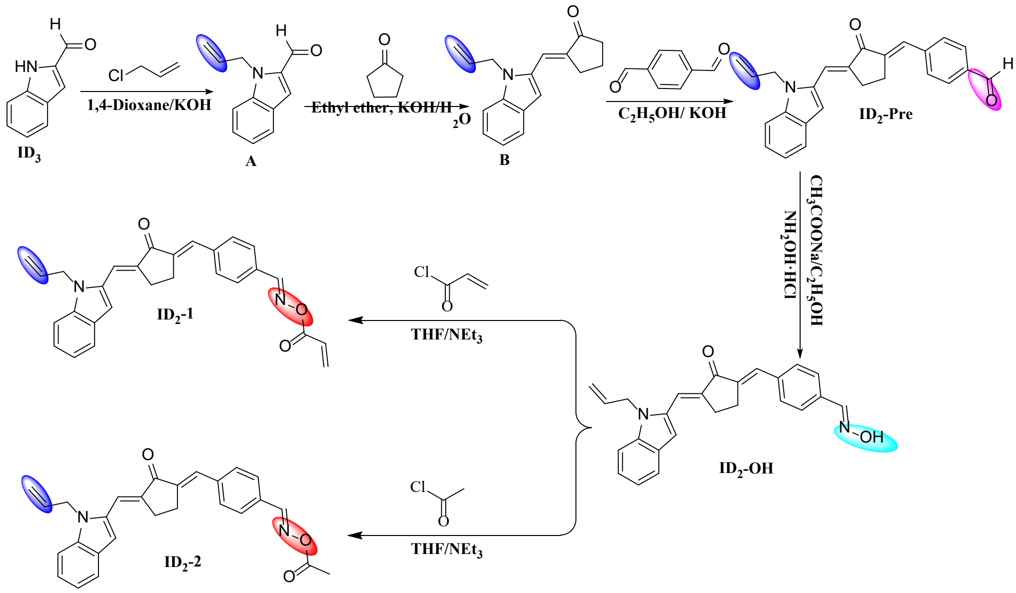

Scheme S1. Synthetic routes of ID_2-Pre, ID_2-OH, ID_2-1 and ID_2-2.

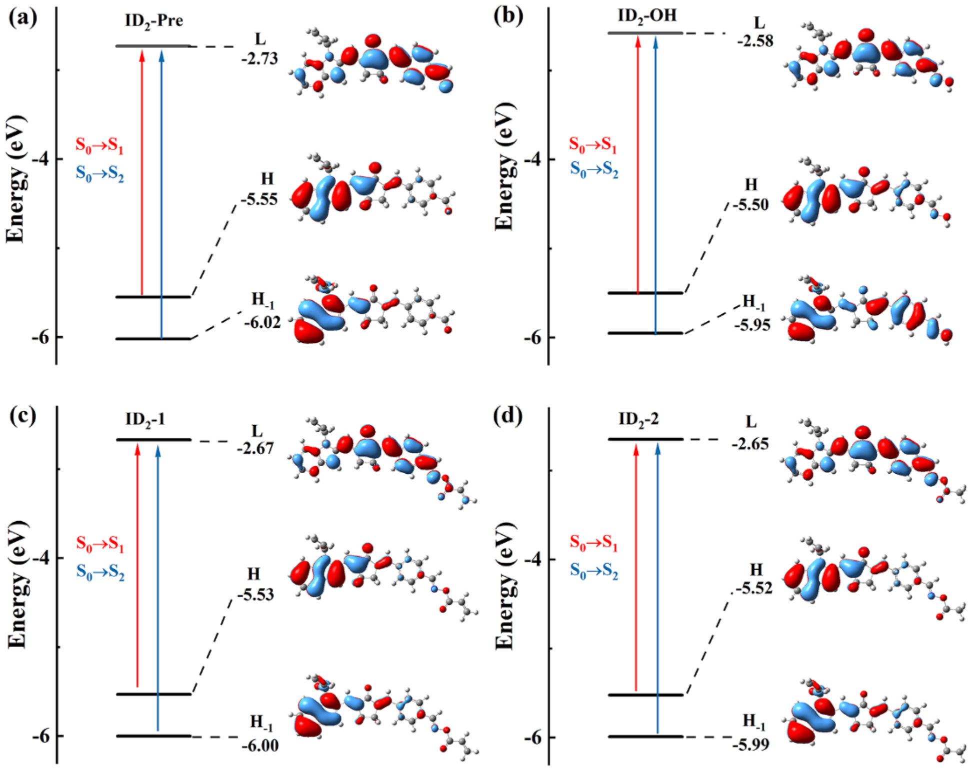

Fig. S1 Frontier molecular orbital diagrams of (a) ID$_2$-Pre, (b) ID$_2$-OH, (c) ID$_2$-1, and (d) ID$_2$-2 with S$_0$→S$_1$, S$_0$→S$_2$ transitions.

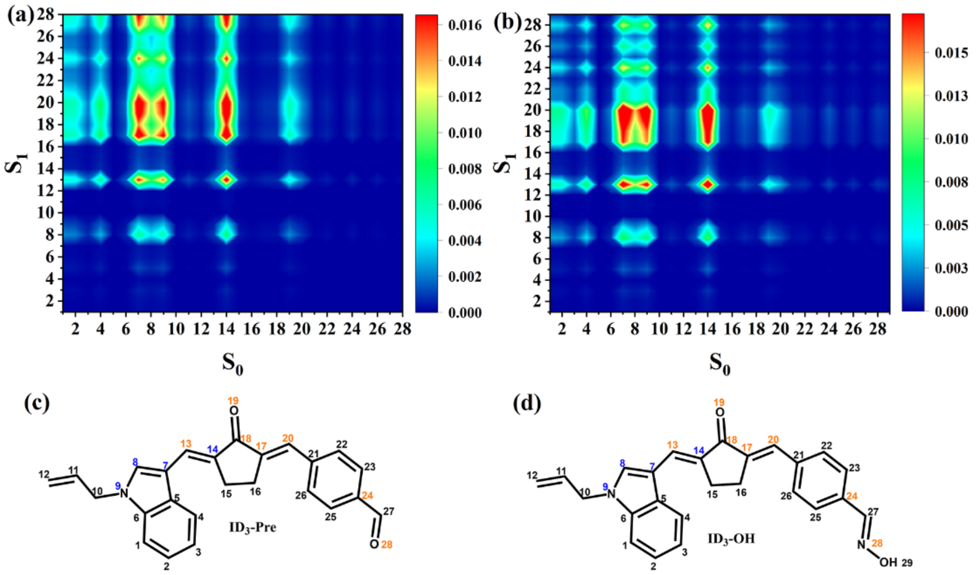

Fig. S2 Transition density matrix of the singlet with the X-axis for S$_0$ and the Y-axis for the S$_1$ of ID$_3$-Pre and ID$_3$-OH. (c-d) Intramolecular electron transfer of ID$_3$-Pre and ID$_3$-OH in the S$_0$–S$_1$ transition.

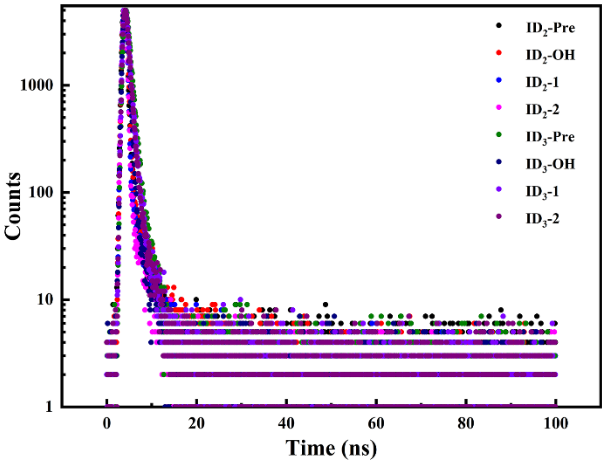

Fig. S3 Lifetime of IDs.

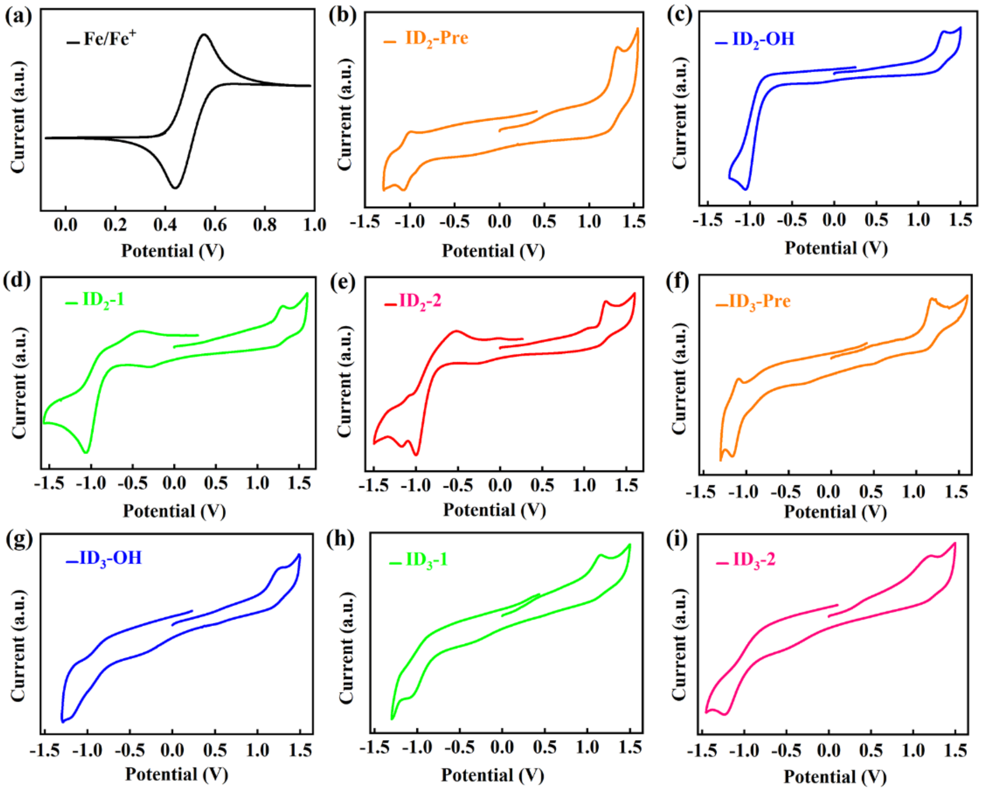

Fig. S4 Cyclic voltammetry curves of IDs (8×10^{-4} mol L^{-1}) in ACN solution which was purged with Ar at room temperature, a platinum electrode at a scan rate of 100 mV s^{-1} with 0.1 M tetrabutylammonium hexafluorophosphate as the supporting electrolyte. The oxidation center of IDs is the N-allylpyrrole part, and the reduction center is the carbonyl part.

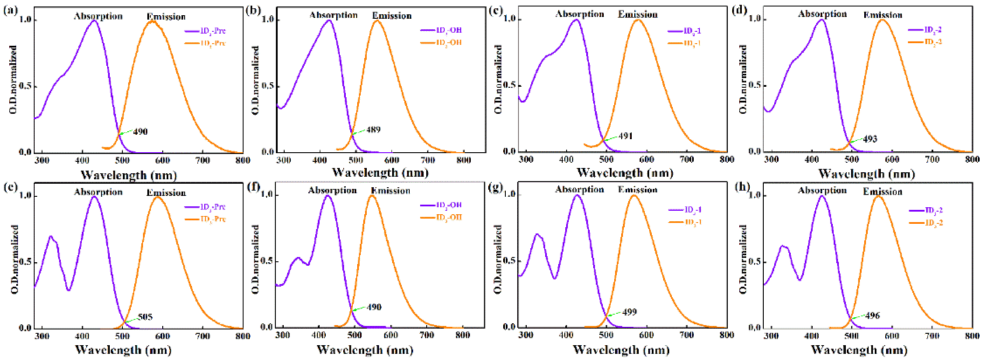

Fig. S5 Normalized UV absorption spectra and fluorescence emission spectra of IDs in acetonitrile.

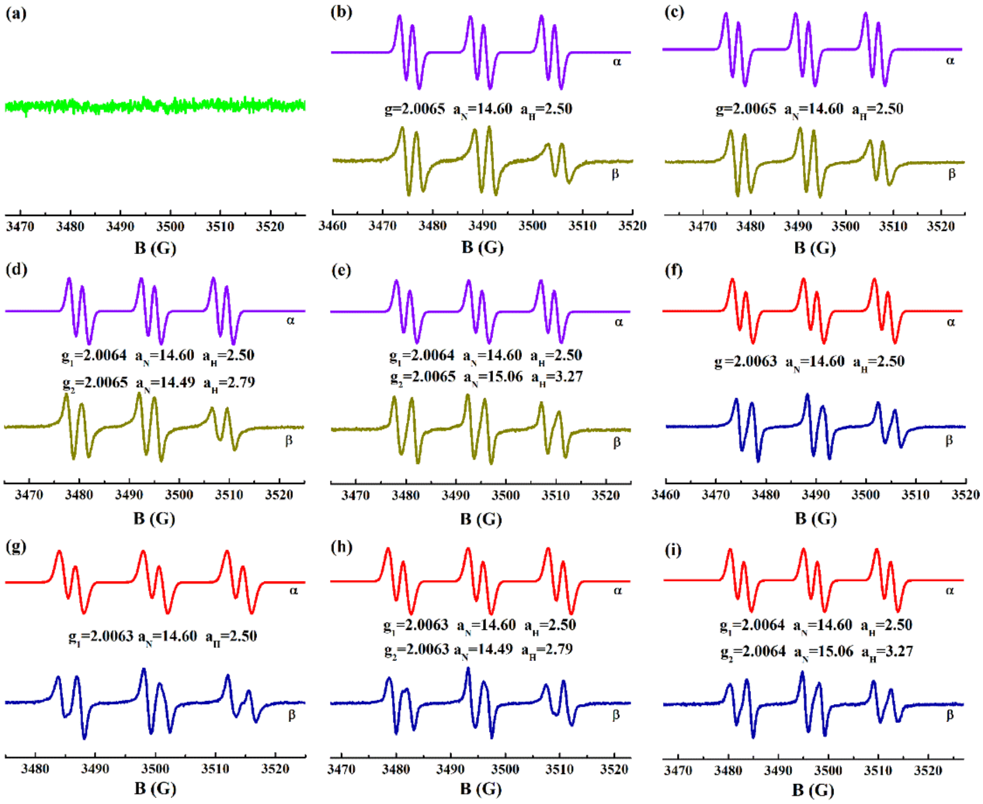

Fig. S6 (a): EPR spin trapping experiments of PBN in tertbutylbenzene upon LED lamp irradiation (room temperature). (b-i): EPR spin trapping experiments of IDs (using PBN in tertbutylbenzene under Ar.) upon LED lamp irradiation (β) experimental and (α) simulated EPR spectra. (b) ID_2-Pre, (c) ID_2-OH, (d) ID_2-1, (e) ID_2-2, (f) ID_3-Pre, (g) ID_3-OH, (h) ID_3-1 and (i) ID_3-2.

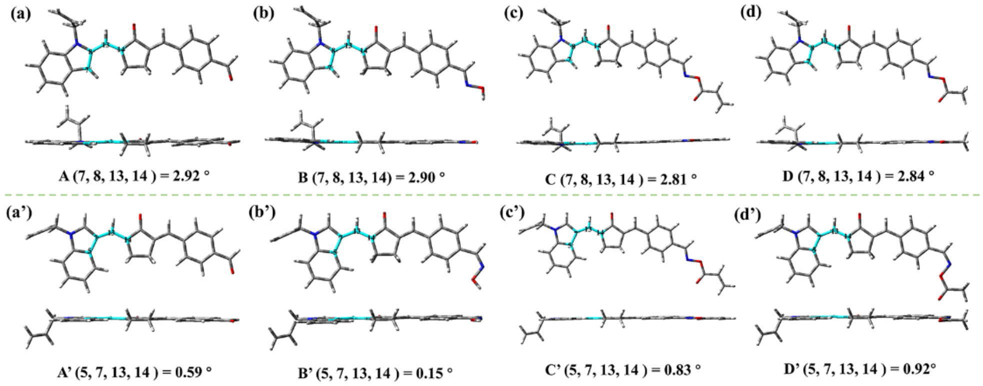

Fig. S7 The excited triplet state geometries of IDs optimized at B3LYP/6-31G(d) level. (a) ID_2-Pre, (b)ID_2-OH, (c)ID_2-1 and (d)ID_2-2; (a') ID_3-Pre, (b') ID_3-OH, (c') ID_3-1 and (d') ID_3-2.

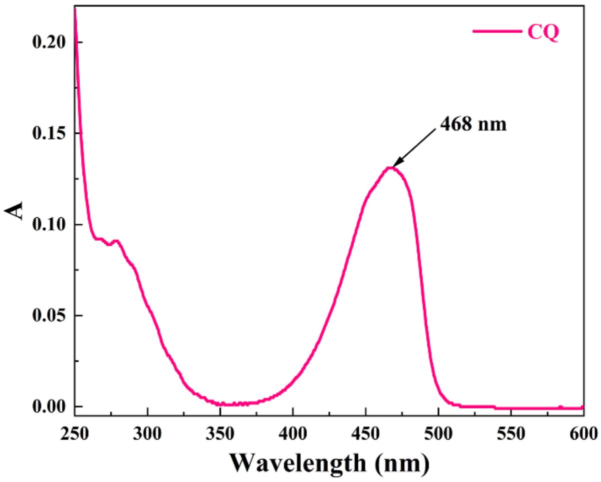

Fig. S8 The UV absorption spectrum of CQ in ACN solution.

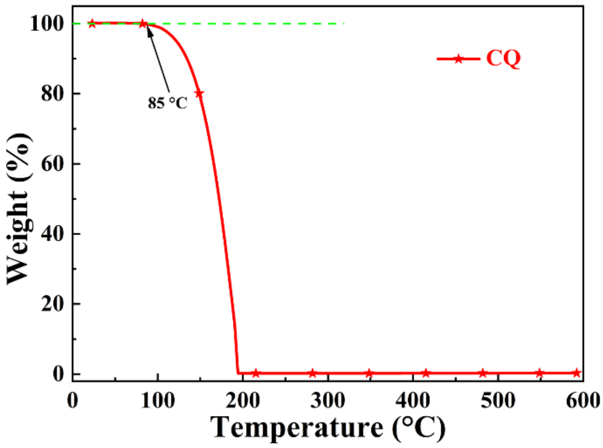

Fig. S9 TG curves of CQ.

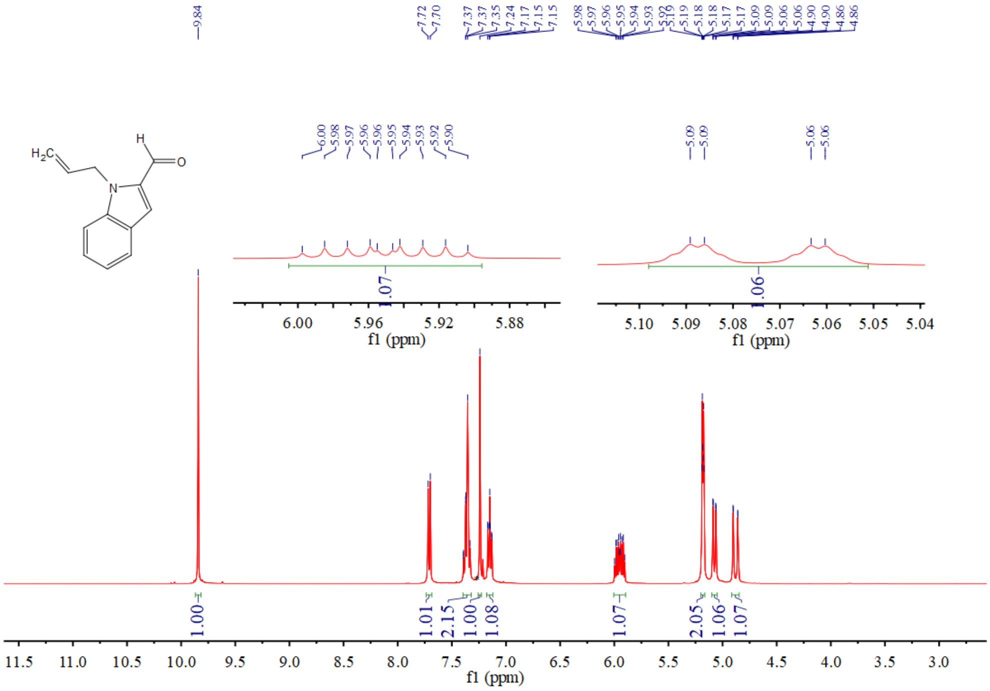

Fig. S10 ^{1}H NMR spectra of **A** (* was $CDCl_3$)

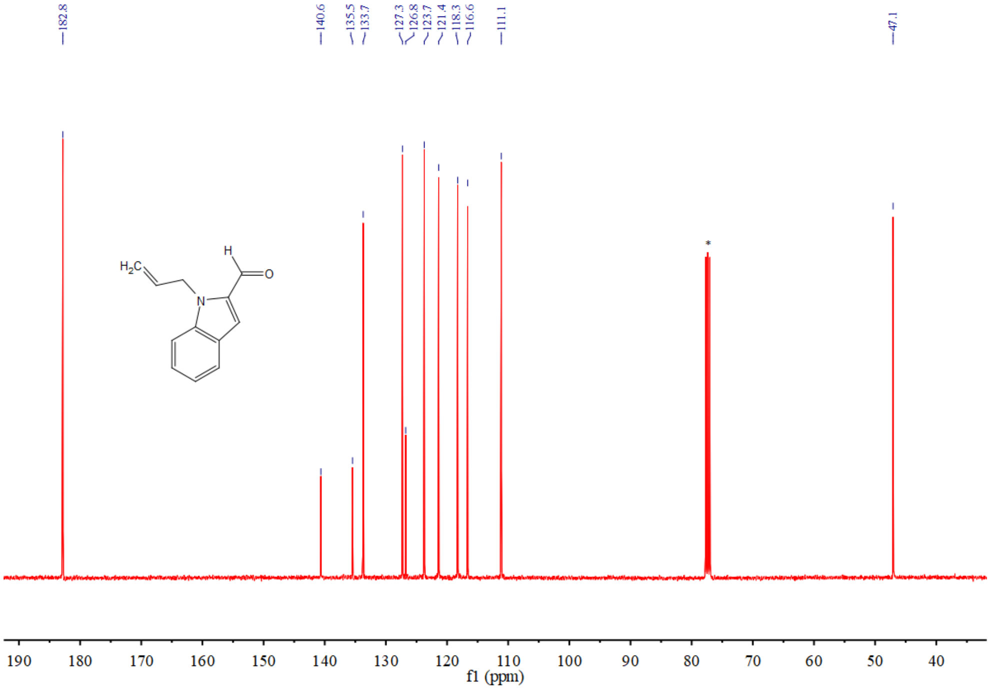

Fig. S11 ^{13}C NMR spectra of **A** (* was $CDCl_3$)

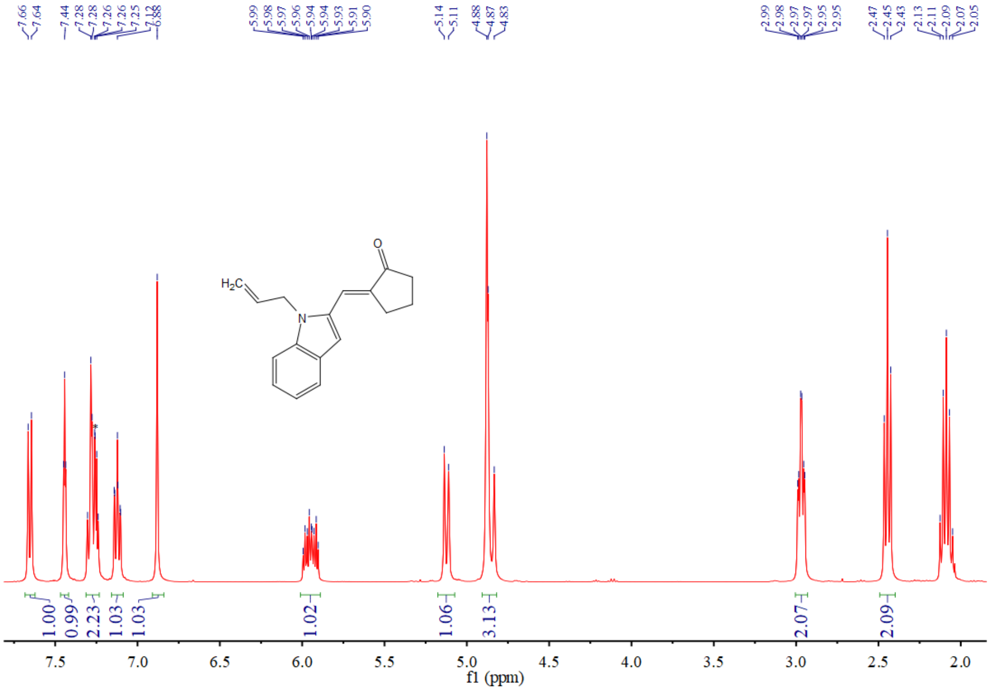

Fig. S12 ^{1}H NMR spectra of **B** (* was $CDCl_3$)

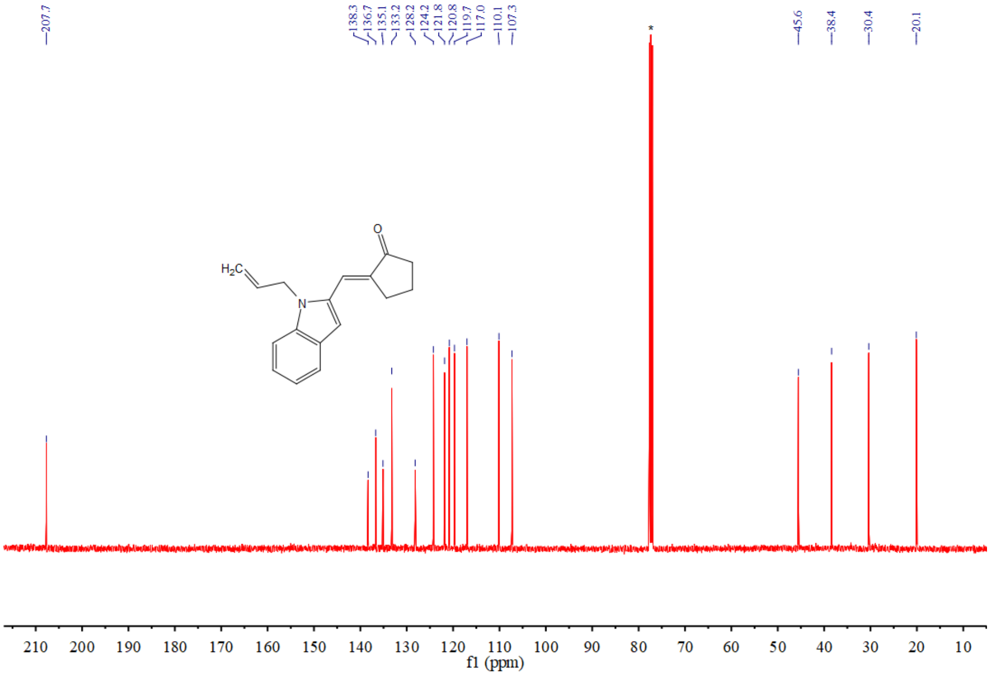

Fig. S13 ^{13}C NMR spectra of **B** (* was $CDCl_3$)

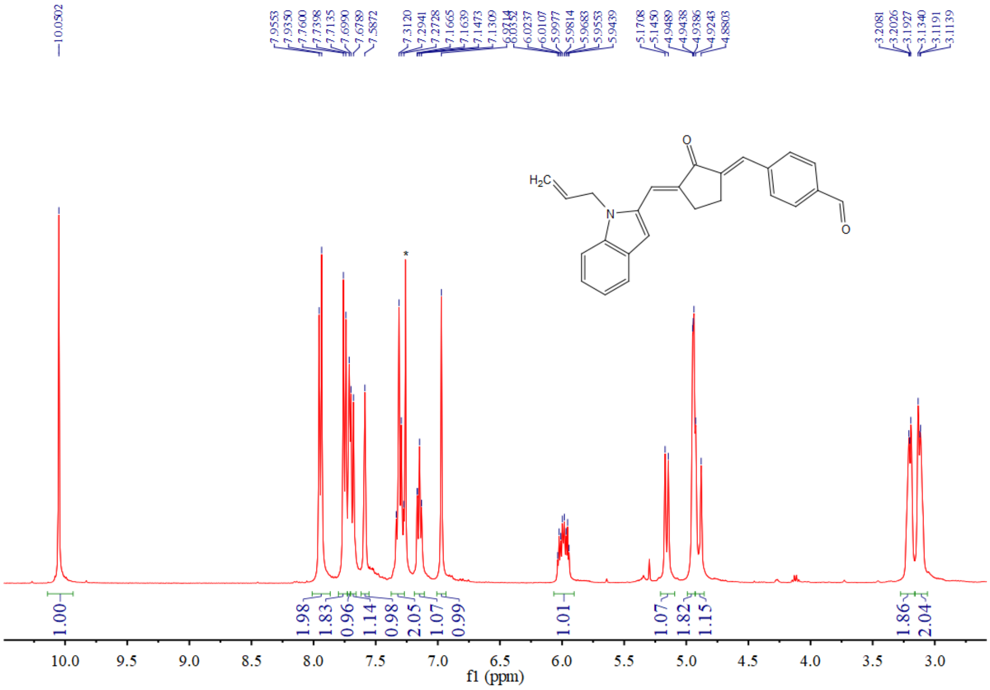

Fig. S14 ^{1}H NMR spectra of **ID$_2$-Pre** (* was CDCl$_3$)

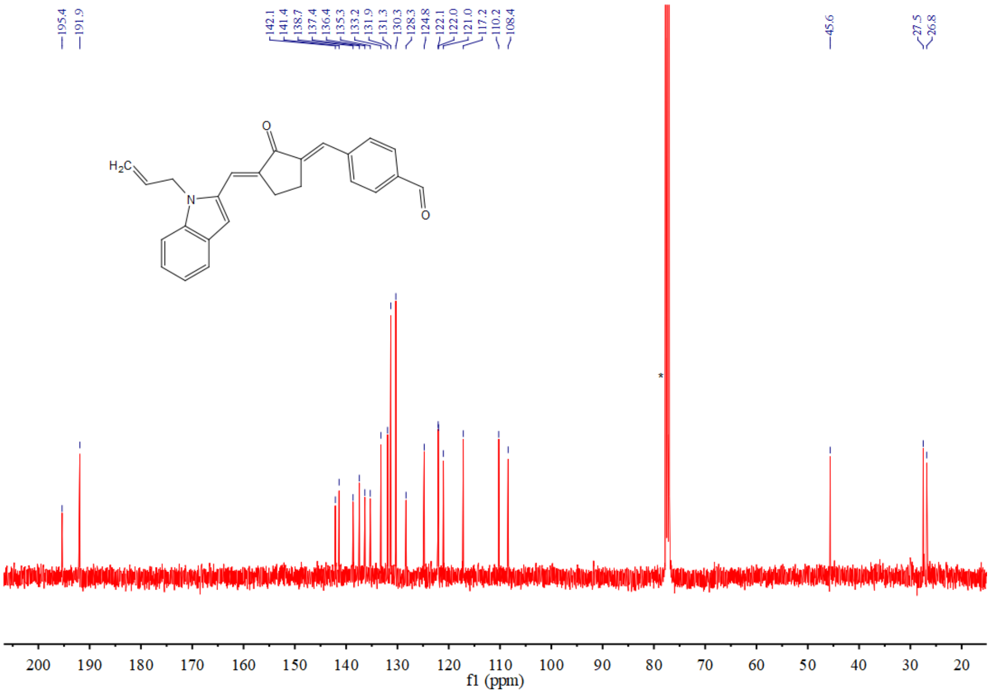

Fig. S15 ^{13}C NMR spectra of **ID$_2$-Pre** (* was CDCl$_3$)

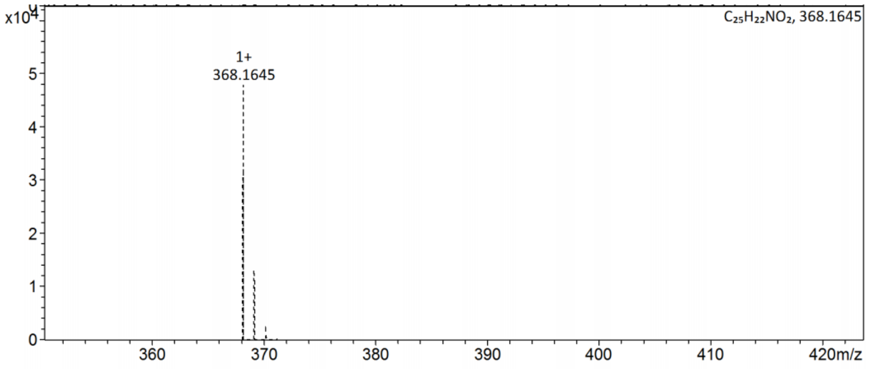

Meas. m/z	#	Ion Formula	Score	m/z	err [mDa]	err [ppm]	mSigma	rdb	e¯ Conf	N-Rule	Adduct
368.164635	1	C25H22NO2	100.00	368.164505	-0.1	-0.4	38.2	15.5	even	ok	M+H

Fig. S16 HR-MS spectra of **ID$_2$-Pre**.

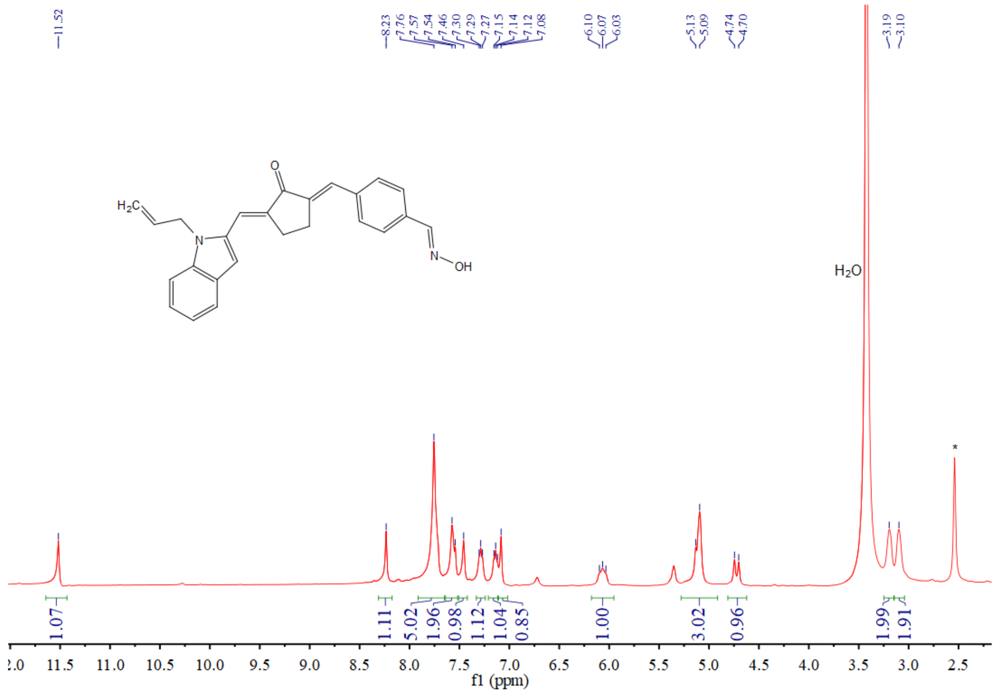

Fig. S17 ^{1}H NMR spectra of **ID$_2$-OH** (* was DMSO-d_6)

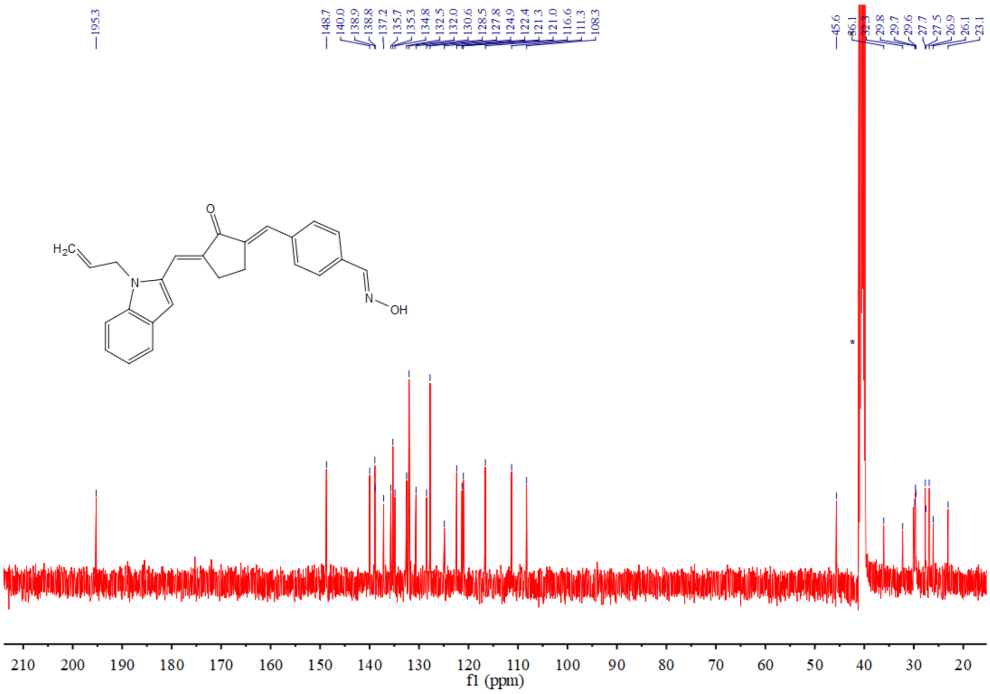

Fig. S18 ^{13}C NMR spectra of **ID$_2$-OH** (* was DMSO-d_6)

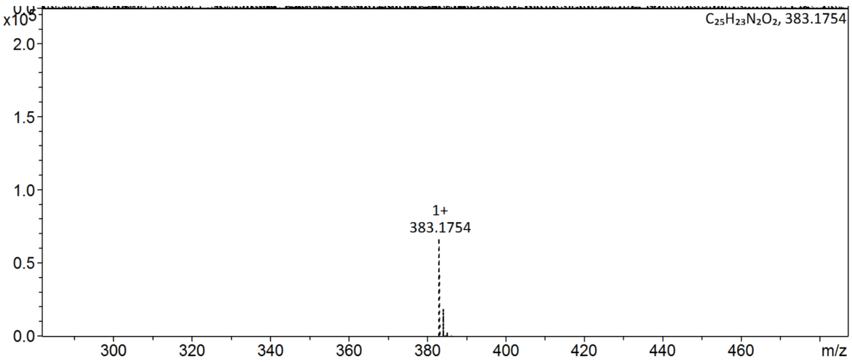

Meas. m/z	#	Ion Formula	Score	m/z	err [mDa]	err [ppm]	mSigma	rdb	e⁻ Conf	N-Rule	Adduct
383.175422	1	C25H23N2O2	100.00	383.175404	-0.0	-0.0	8.3	15.5	even	ok	M+H

Fig. S19 HR-MS spectra of **ID$_2$-OH**.

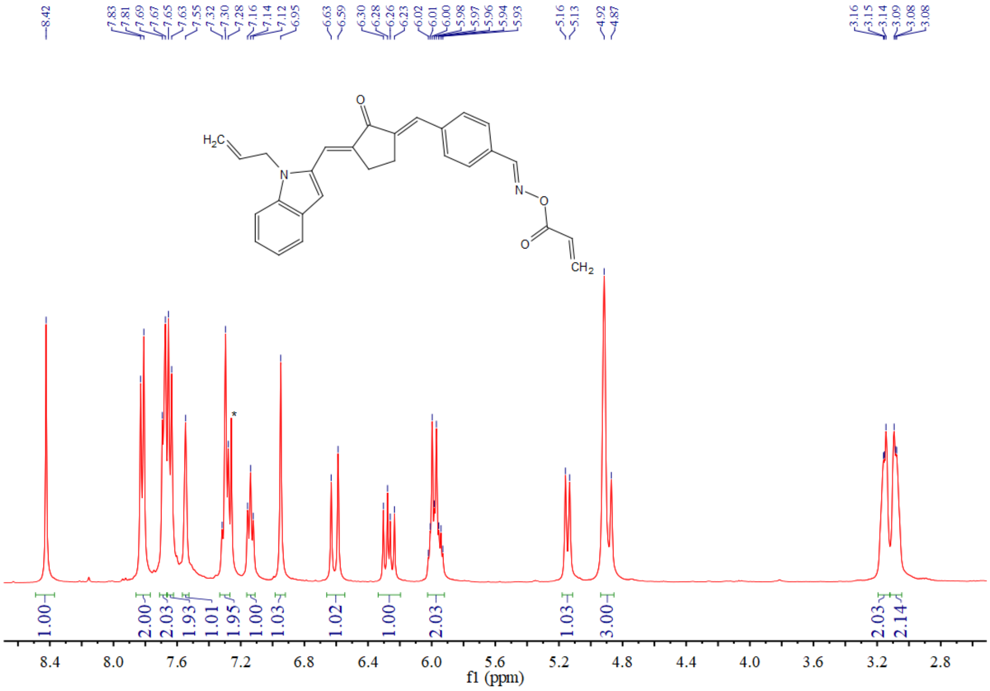

Fig. S20 ^{1}H NMR spectra of **ID$_2$-1** (* was CDCl$_3$)

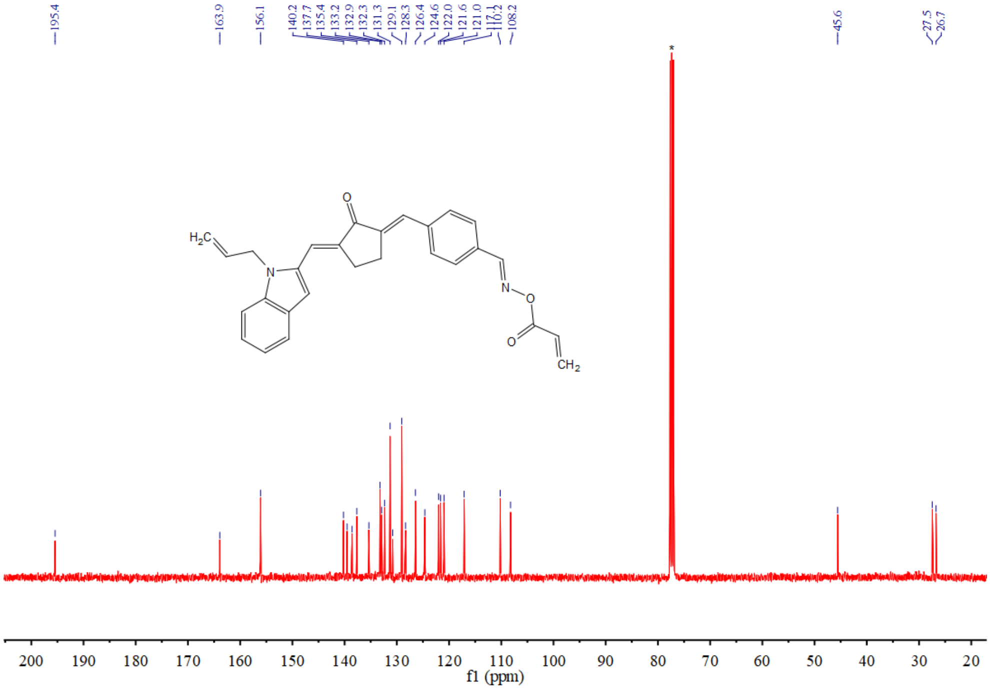

Fig. S21 ^{13}C NMR spectra of **ID$_2$-1** (* was CDCl$_3$)

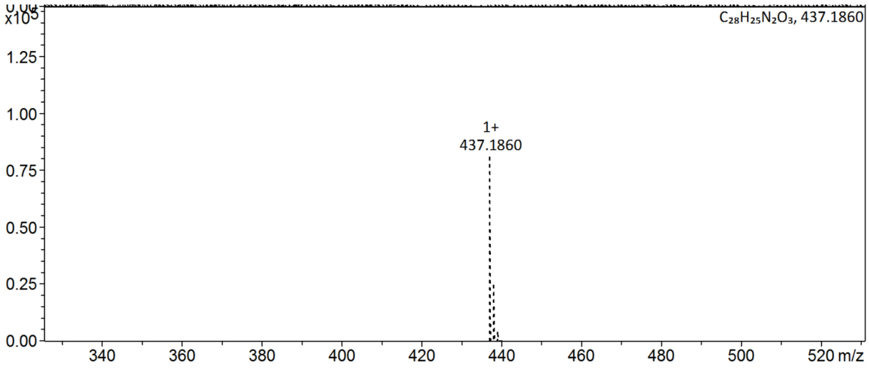

Meas. m/z	#	Ion Formula	Score	m/z	err [mDa]	err [ppm]	mSigma	rdb	e⁻ Conf	N-Rule	Adduct
437.188076	1	C28H25N2O3	100.00	437.185969	-2.1	-4.8	8.7	17.5	even	ok	M+H

Fig. S22 HR-MS spectra of **ID$_2$-1**.

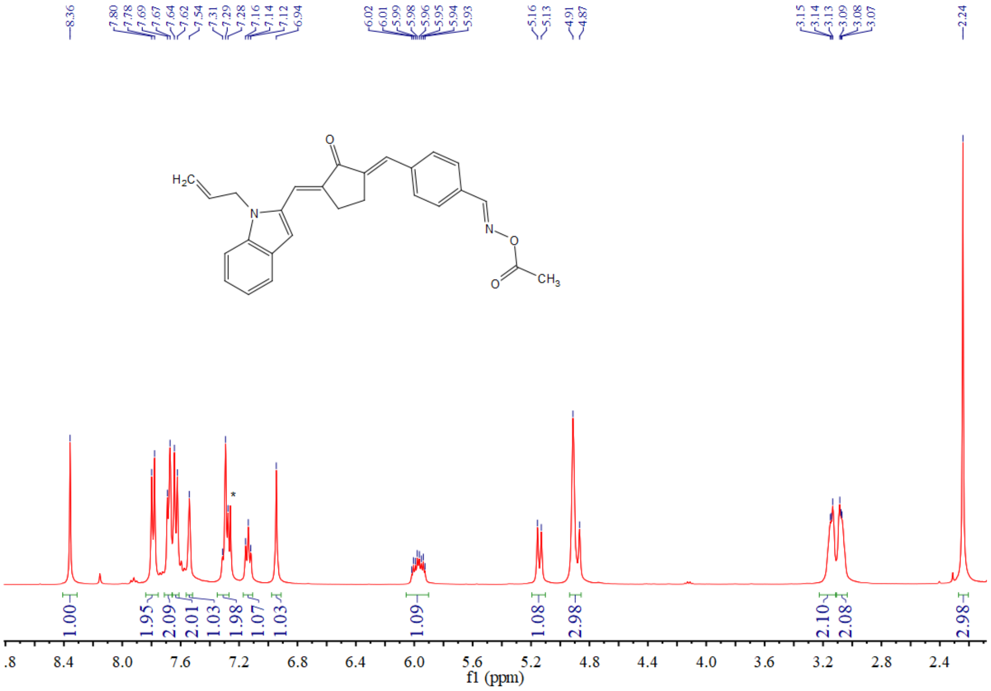

Fig. S23 ^{1}H NMR spectra of **ID$_2$-2** (* was $CDCl_3$).

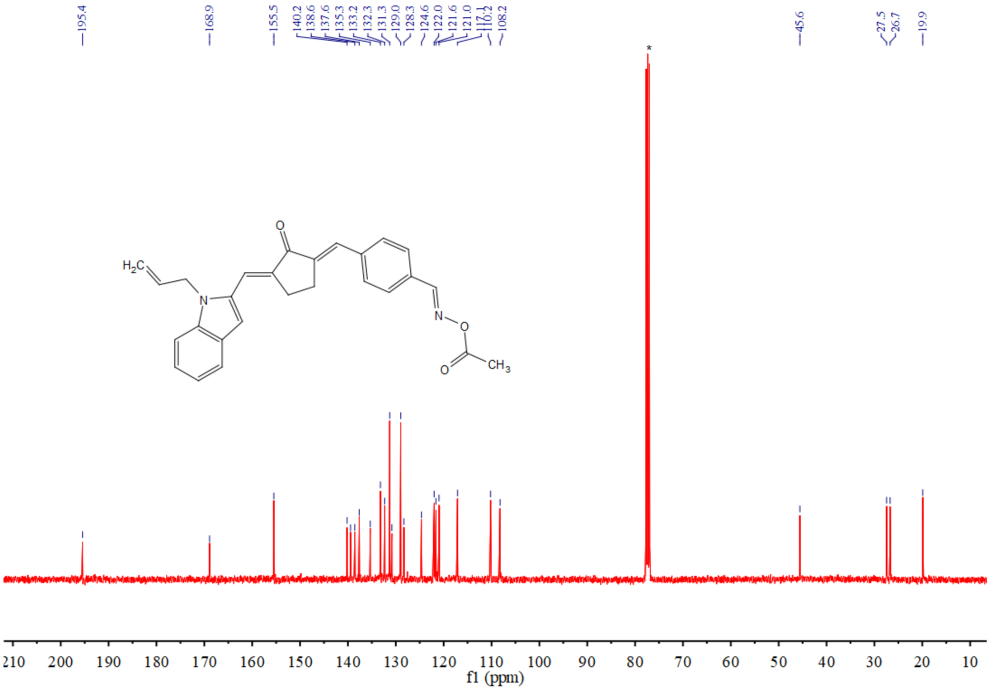

Fig. S24 ^{13}C NMR spectra of **ID$_2$-2** (* was CDCl$_3$).

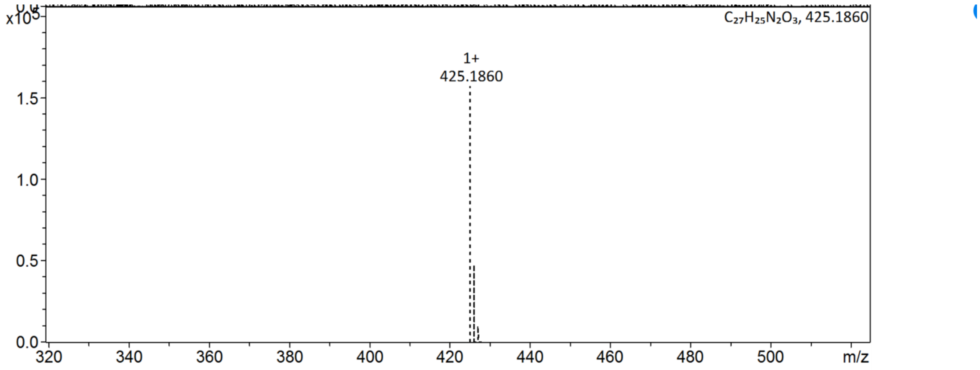

Meas. m/z	#	Ion Formula	Score	m/z	err [mDa]	err [ppm]	mSigma	rdb	e⁻ Conf	N-Rule	Adduct
425.186111	1	C27H25N2O3	100.00	425.185969	-0.1	-0.3	5.4	16.5	even	ok	M+H

Fig. S25 HR-MS spectra of **ID$_2$-2**.

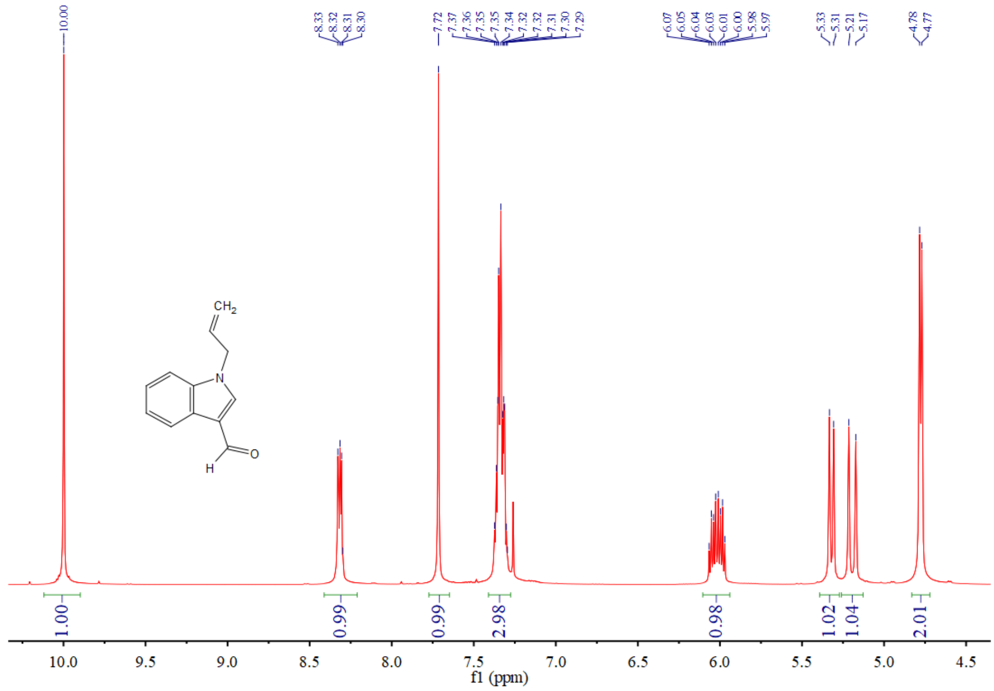

Fig. S26 ^{1}H NMR spectra of **C** (* was $CDCl_3$).

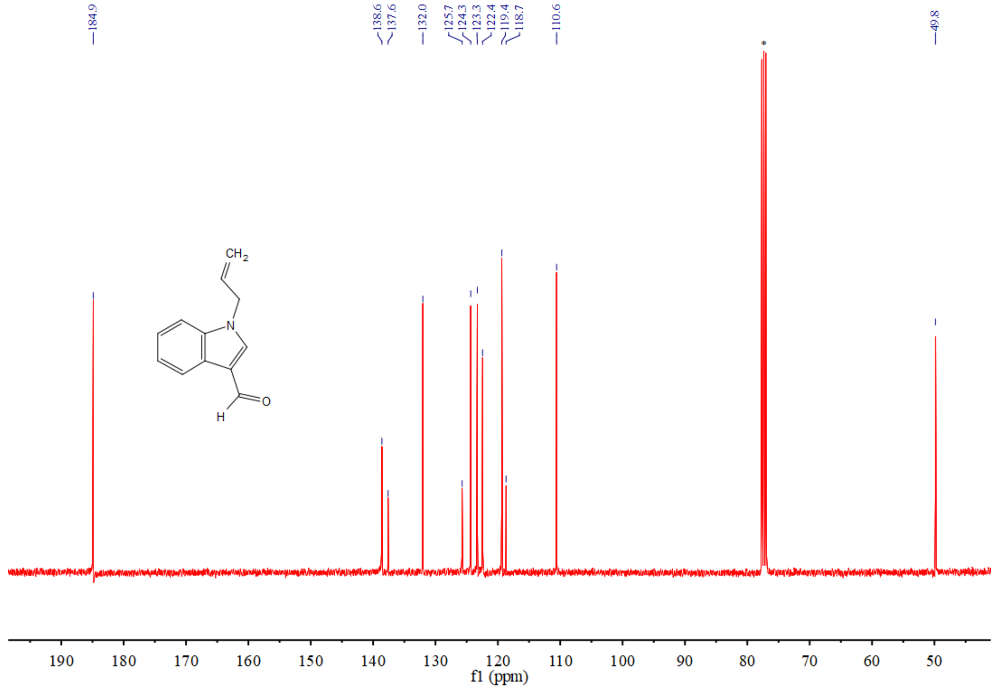

Fig. S27 ^{13}C NMR spectra of **C** (* was $CDCl_3$).

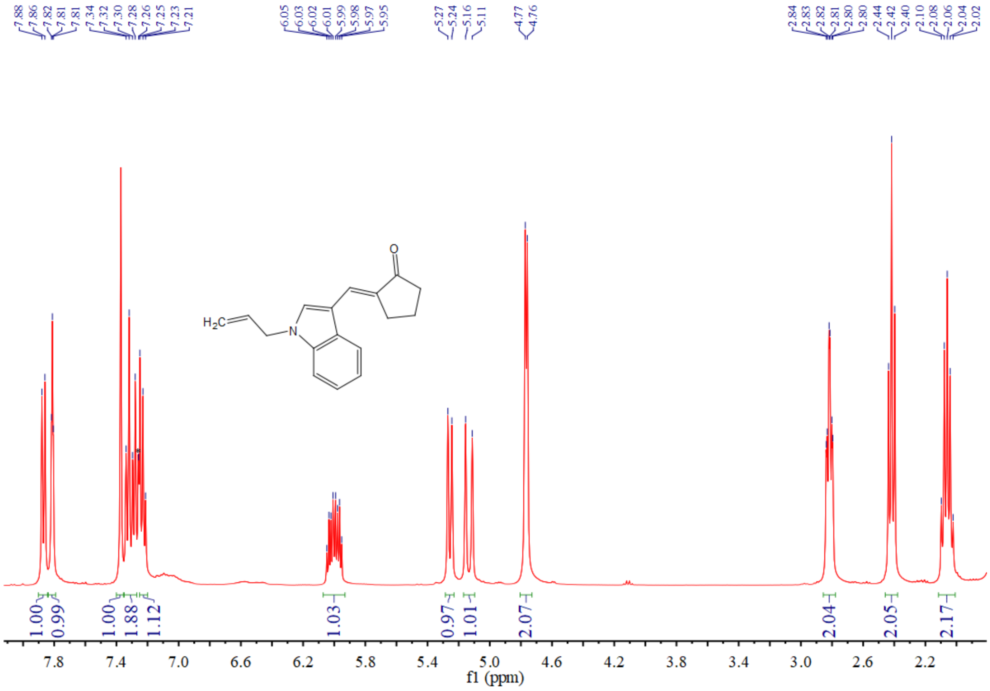

Fig. S28 ^{13}C NMR spectra of **D** (* was $CDCl_3$).

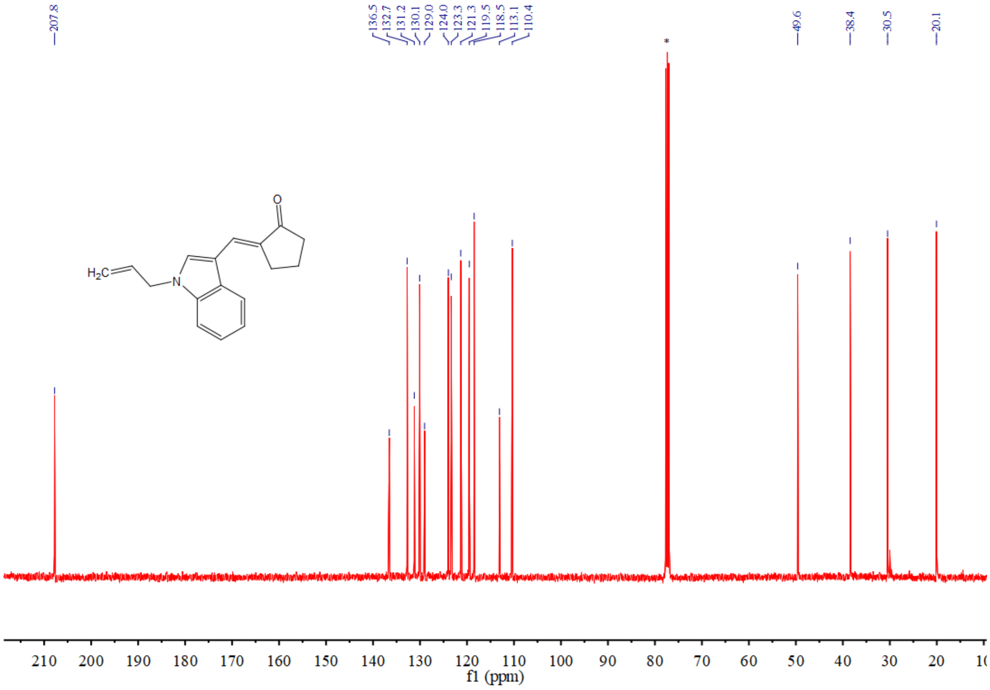

Fig. S29 ^{13}C NMR spectra of **D** (* was $CDCl_3$).

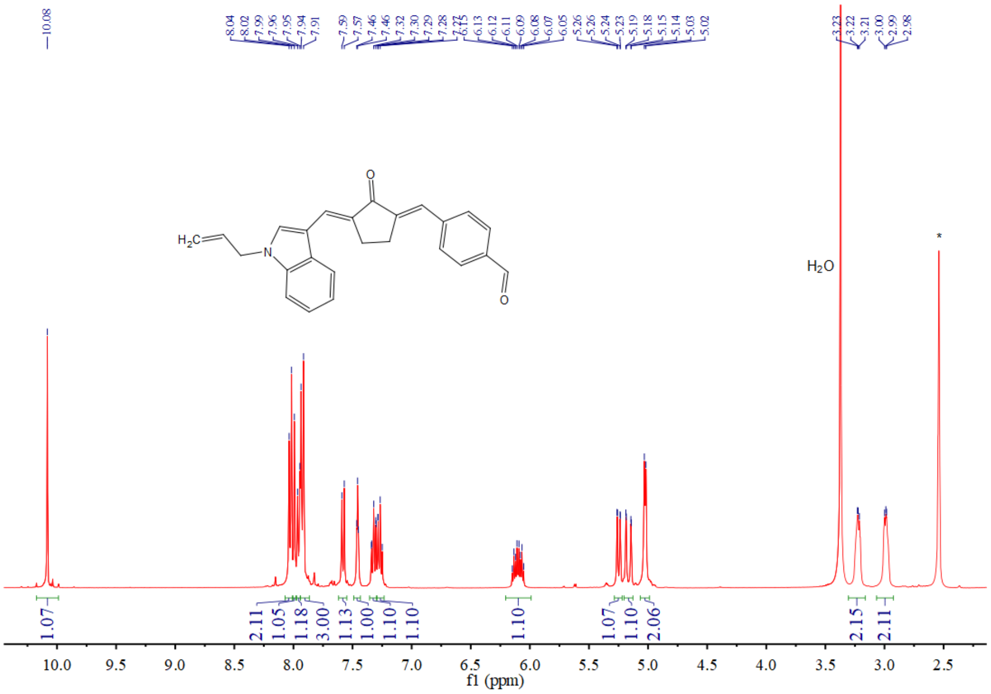

Fig. S30 ^{1}H NMR spectra of **ID$_3$-Pre** (* was DMSO-*d$_6$*).

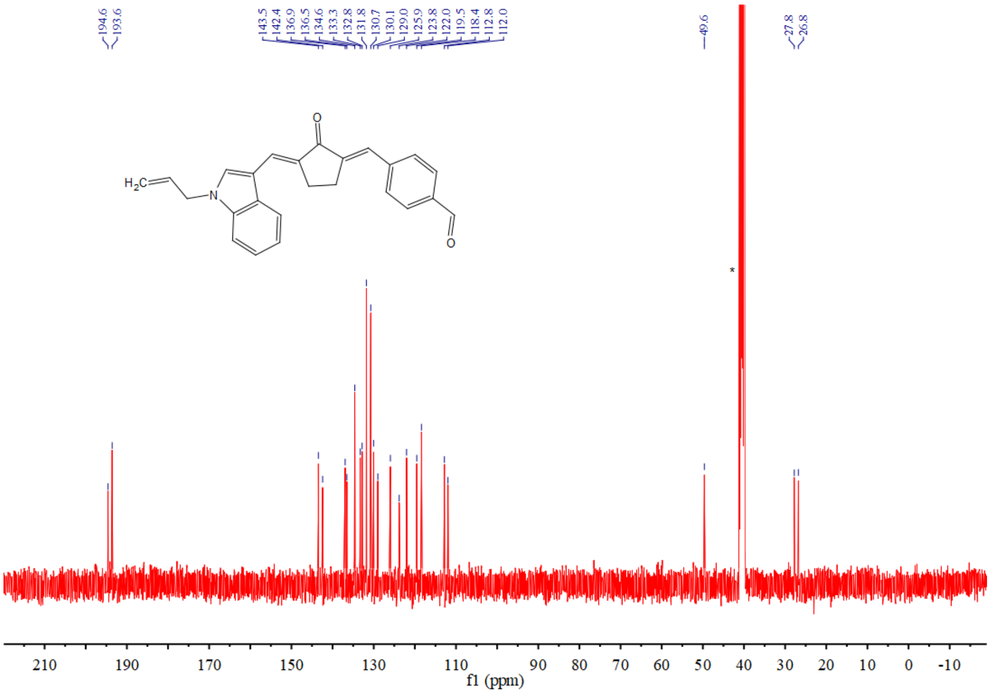

Fig. S31 ^{13}C NMR spectra of **ID$_3$-Pre** (* was DMSO-*d$_6$*).

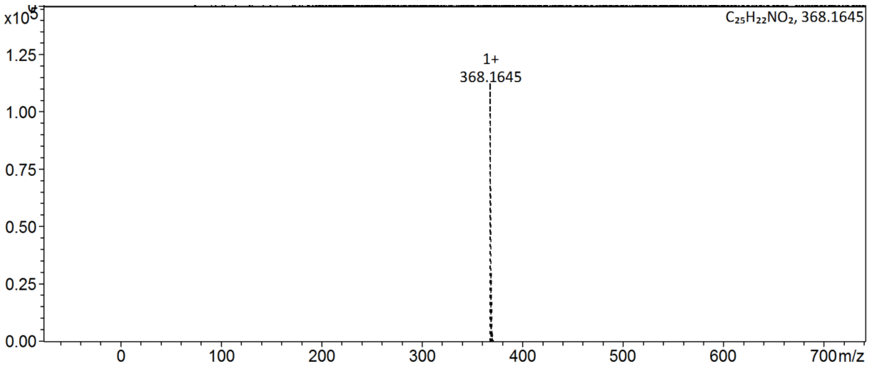

Meas. m/z	#	Ion Formula	Score	m/z	err [mDa]	err [ppm]	mSigma	rdb	e⁻ Conf	N-Rule	Adduct
368.164384	1	C25H22NO2	100.00	368.164505	0.1	0.3	3.4	15.5	even	ok	M+H

Fig. S32 HR-MS spectra of **ID$_3$-Pre**.

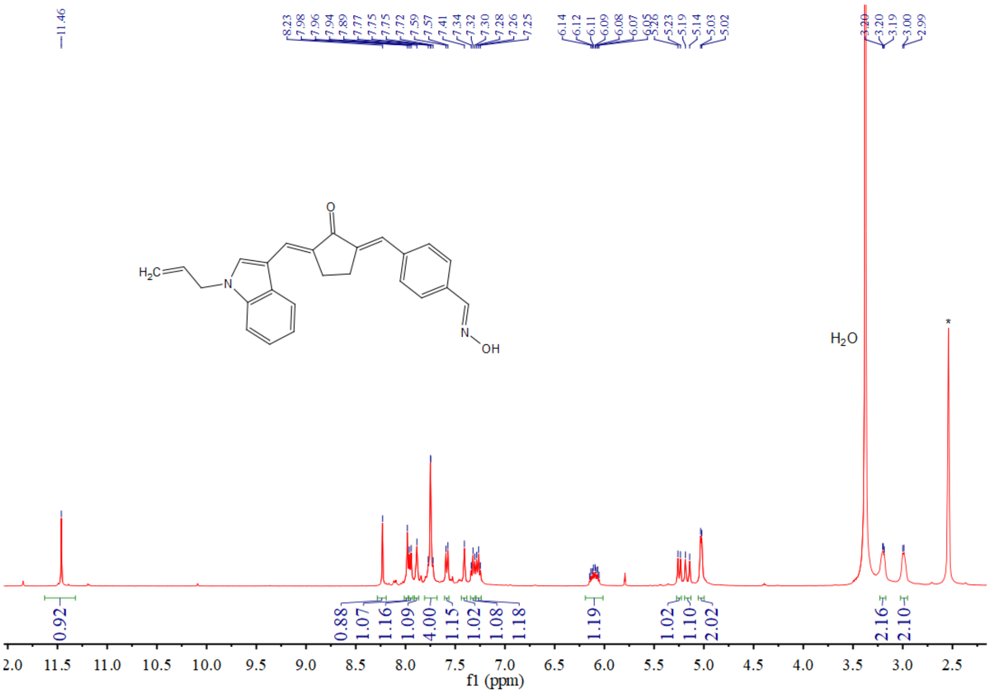

Fig. S33 ^{1}H NMR spectra of **ID$_3$-OH** (* was DMSO-d_6)

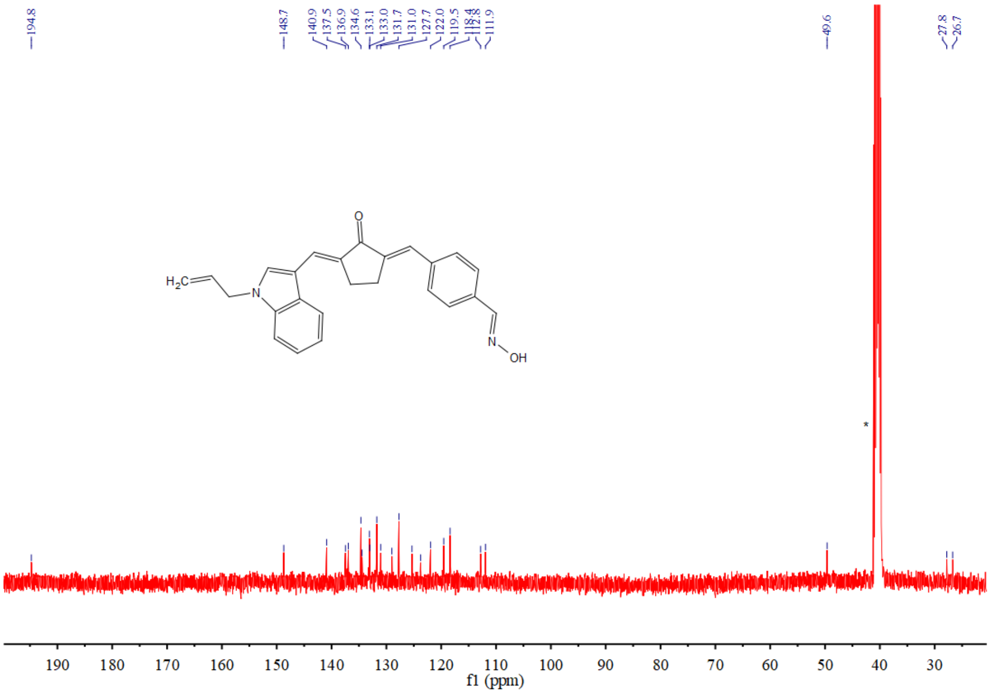

Fig. S34 ^{13}C NMR spectra of **ID$_3$-OH** (* was DMSO-d_6)

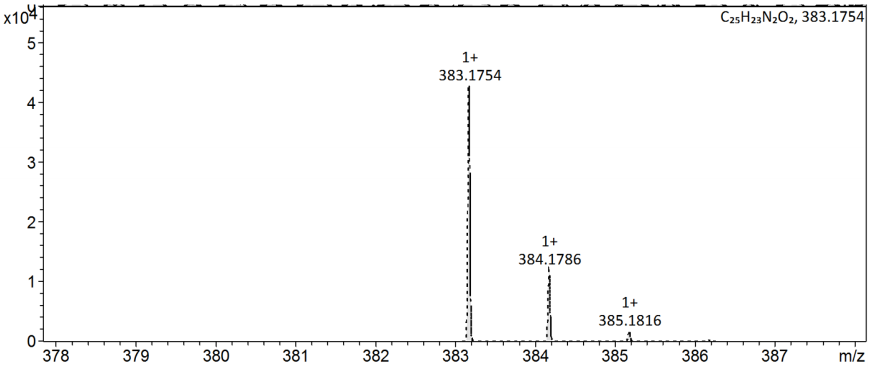

Meas. m/z	#	Ion Formula	Score	m/z	err [mDa]	err [ppm]	mSigma	rdb	e⁻ Conf	N-Rule	Adduct
383.175177	1	C25H23N2O2	100.00	383.175404	0.2	0.6	25.9	15.5	even	ok	M+H

Fig. S35 HR-MS spectra of **ID$_3$-OH**.

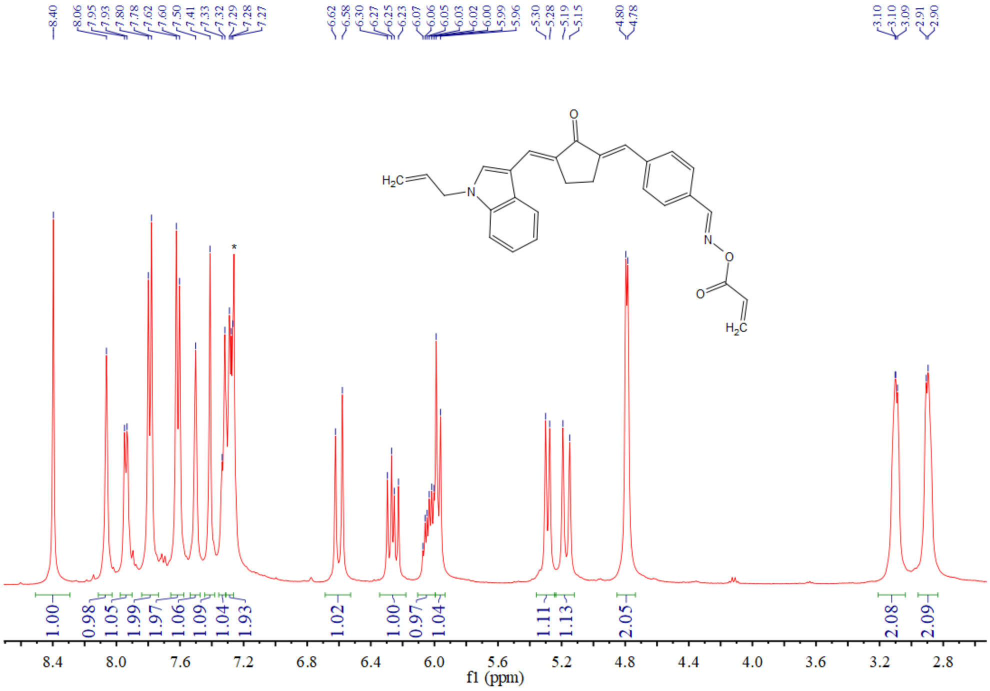

Fig. S36 ^{1}H NMR spectra of **ID$_3$-1** (* was CDCl$_3$)

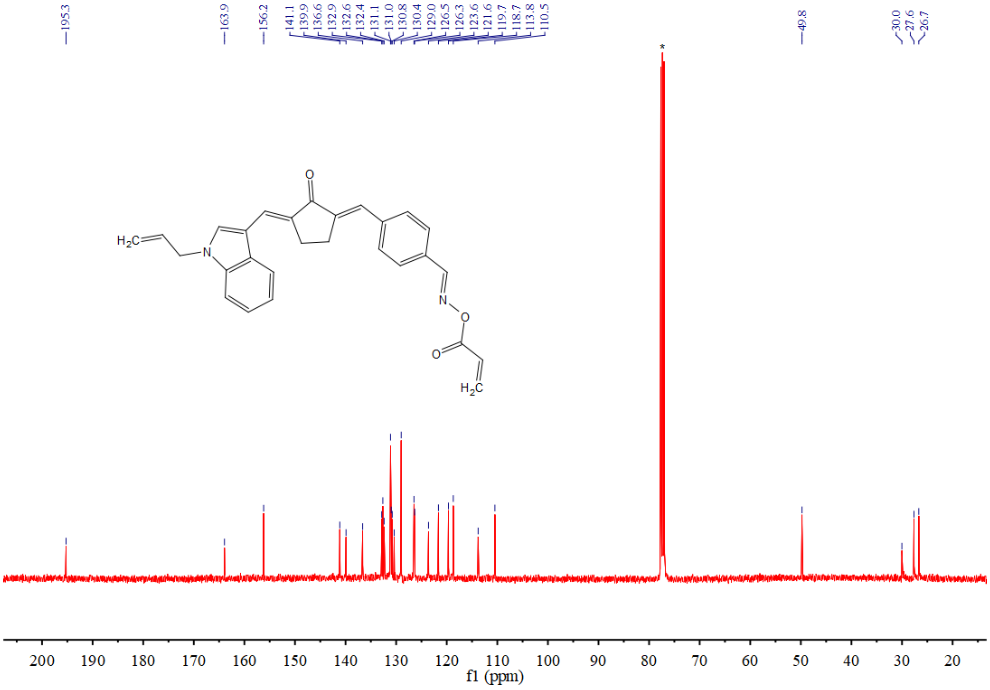

Fig. S37 ^{13}C NMR spectra of **ID$_3$-1** (* was CDCl$_3$)

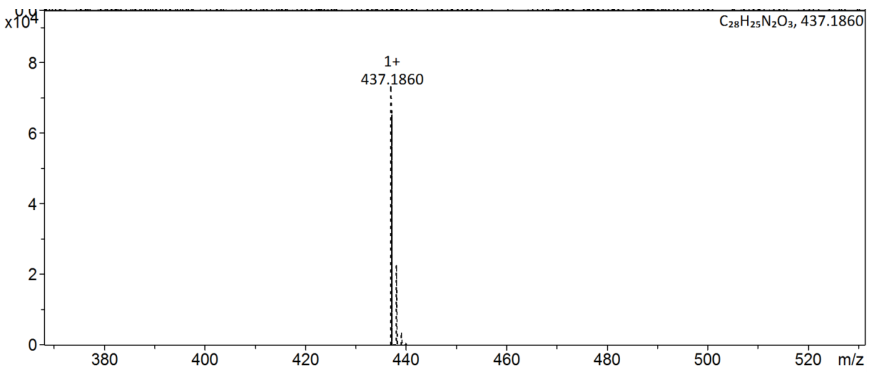

Meas. m/z	#	Ion Formula	Score	m/z	err [mDa]	err [ppm]	mSigma	rdb	e⁻ Conf	N-Rule	Adduct
437.188043	1	C28H25N2O3	100.00	437.185969	-2.1	-4.7	10.6	17.5	even	ok	M+H

Fig. S38 HR-MS spectra of **ID$_3$-1**.

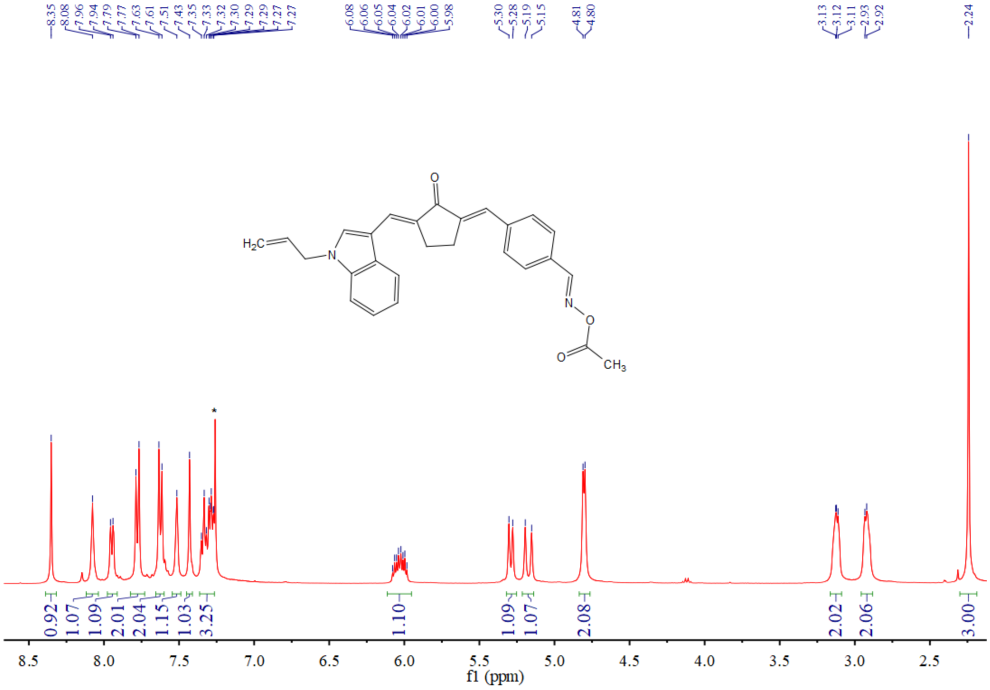

Fig. S39 ^{1}H NMR spectra of **ID$_3$-2** (* was $CDCl_3$)

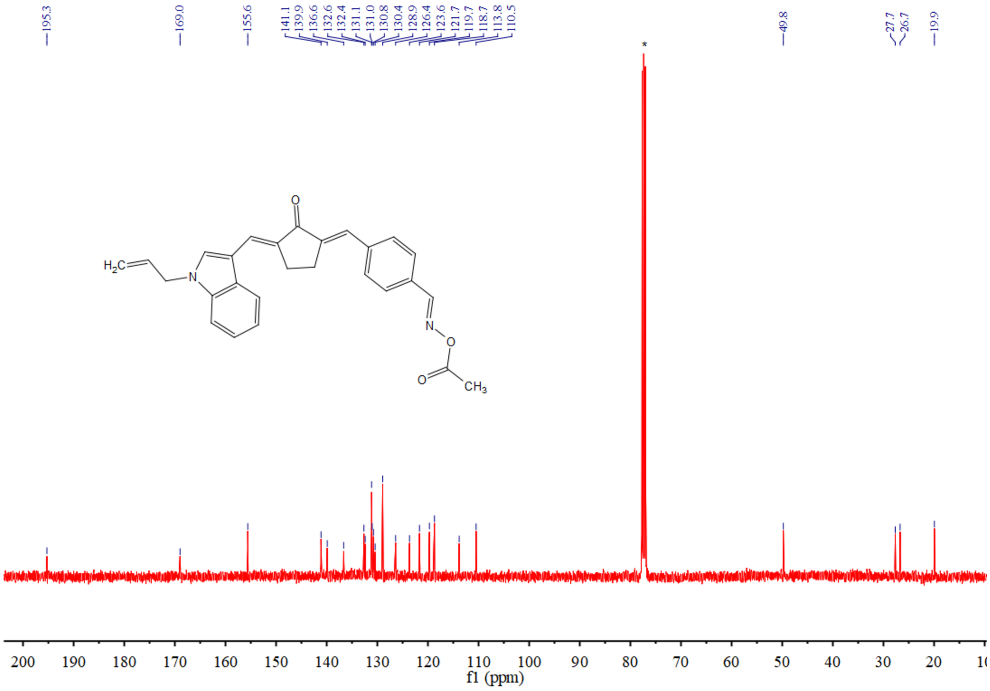

Fig. S40 ^{13}C NMR spectra of **ID$_3$-2** (* was CDCl$_3$)

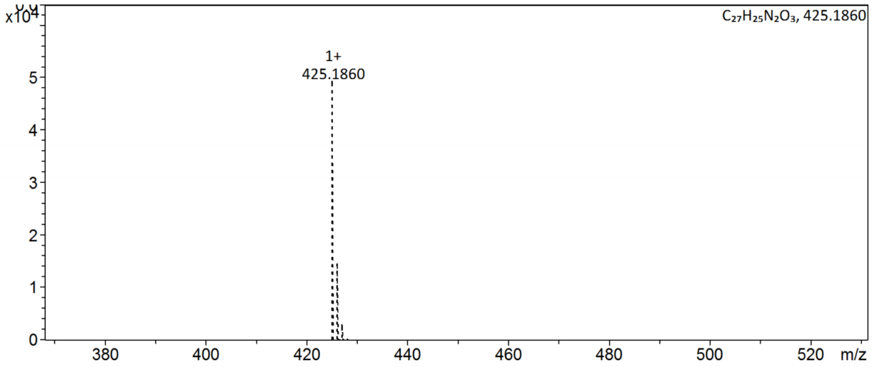

Meas. m/z	#	Ion Formula	Score	m/z	err [mDa]	err [ppm]	mSigma	rdb	e⁻ Conf	N-Rule	Adduct
425.186537	1	C27H25N2O3	100.00	425.185969	-0.6	-1.3	29.5	16.5	even	ok	M+H

Fig. S41 HR-MS spectra of **ID$_3$-2**.

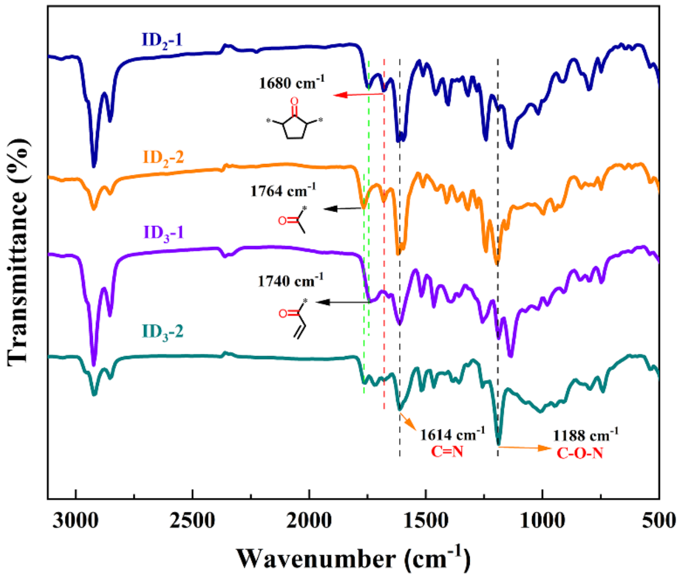

Fig. S42 FT-IR spectra of **IDs**.

The detailed photopolymerization results

From Fig. S43(a), photopolymer exhibits two new signals at 170-180 ppm (1) and 42 ppm (2) compared with the HDDA monomer. Signal 1and 2 can be attributed to carbonyl carbon (**C**=O) and its α-position methylene carbon (C=O**C**H$_2$-), respectively, demonstrating that the bifunctional HDDA initiated by ID$_3$-2 forms the photopolymer with network structure. Based on the solid-state ^{13}C NMR result and the final double bond conversion of 84% when HDDA is initiated by ID$_3$-2, the molecular formula of the photopolymer is guessed as shown in Fig. S43(b). From the TG-DSC curves (Fig. S43(c-d)), the photopolymer formed by ID$_3$-2 initiated HDDA under LED@405 nm irradiation exhibits thermal stability that there is less residual free HDDA to form a stable cross-linking structure with slower decomposition.

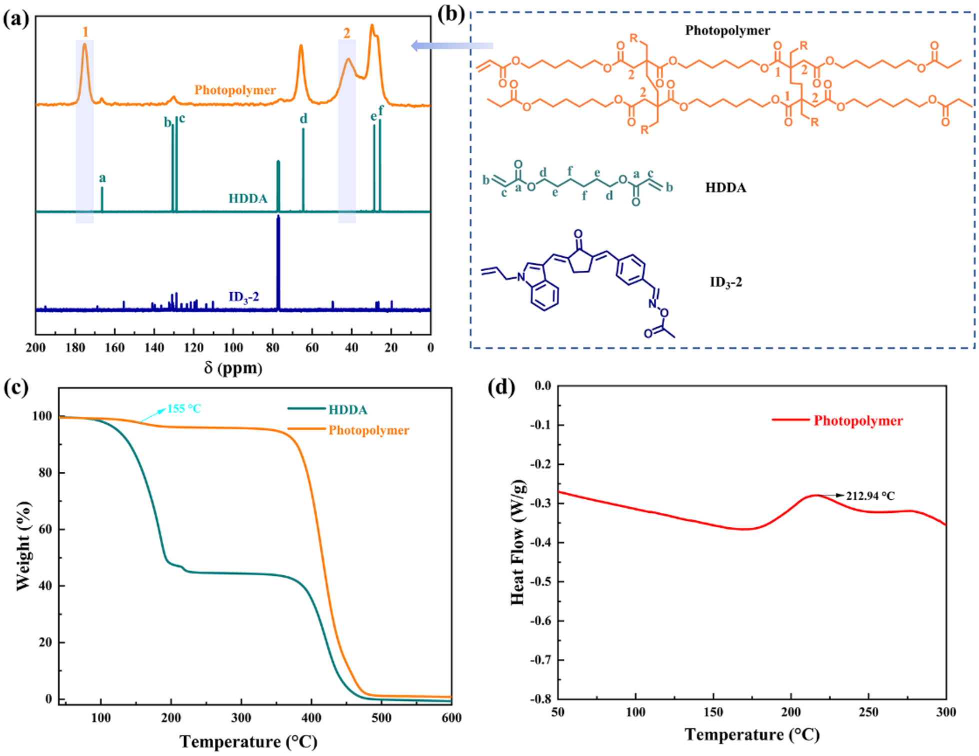

Fig. S43 (a) ^{13}C solid-state NMR spectra of Photopolymer, and liquid ^{13}C NMR of HDDA and ID$_3$-2 in CDCl$_3$; (b): Molecular formulas of ID$_3$-2, HDDA and photopolymer; (c) TG and (d) DSC curve of photopolymer. (Photopolymer obtained by ID$_3$-2 initiated HDDA under illumination. ID$_3$-2=1×10^{-5} mol g^{-1}, I_{405}=45 mW cm^{-2}).

Thermal initiating ability of IDs

The N-O bond in oxime ester compound has been proved to be decomposed easily upon heating [6], and the excellent thermal stability facilitates the long-term storage of PIs.[7] Therefore, the thermal stability of IDs was evaluated using the TG-DTG test. The initial thermal decomposition temperatures (TDTs) of ID$_2$-Pre, ID$_2$-OH, ID$_2$-1 and ID$_2$-2 are 192.41 °C, 131.15 °C, 135.60 °C, and 133.87 °C, respectively (Fig. S44(a) and S44(e)), and the fastest TDTs are 408.80 °C, 401.88 °C, 389.53 °C, and 388.30 °C, respectively. As shown in Fig. S44(b) and S44(f), the onset TDTs of ID$_3$-Pre, ID$_3$-OH, ID$_3$-1, and ID$_3$-2 are 237.37 °C, 138.56 °C, 123.74 °C, and 132.14 °C, respectively, and the fastest TDTs are almost identical, 413.27 °C, 406.90 °C, 399.06 °C and 400.52 °C, respectively. The results exhibit that IDs are stable at 140 °C, and do not start to decompose until approximately 150 °C. Moreover, the TDTs of IDs are significantly higher than that of commercial CQ (T_{decomp}=85 °C, Fig. S9), which displays that the prepared IDs possess superior thermal stability and could meet the requirements for long-term temperature-resistant applications and storage. In addition, TG-DTG curves of IDs initiated HDDA polymeric materials are used to further evaluate the practical application effects and thermal stability (Fig. S44(c-d) and S44(g-h)). Interestingly, all polymeric materials start to decompose only above 200 °C, demonstrating the outstanding thermal stability, which also proves that the thermal stability of IDs is further enhanced after involving the polymerization reaction. Collectively, all IDs reveal good thermal and polymerization stability, which is beneficial for storage and transportation.

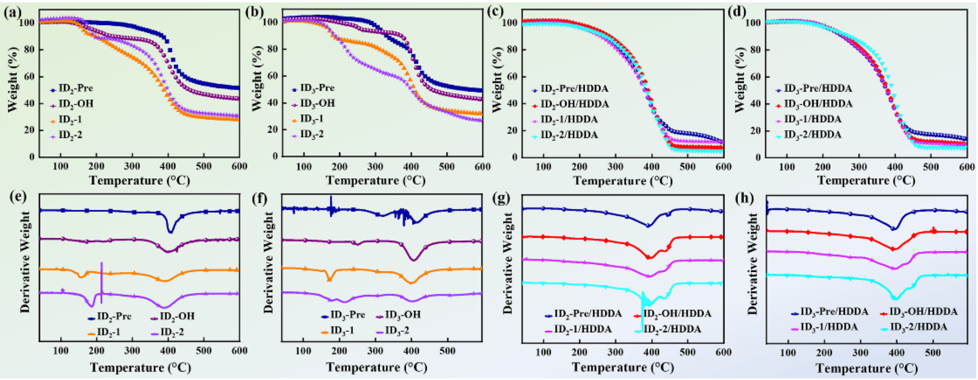

Fig. S44 (a-h) TG-DSC curves of IDs and IDs/HDDA. (IDs/HDDA obtained by ID_3-2 initiated HDDA under Xenon Lamp. $ID_3\text{-}2=1\times10^{-5}$ mol g^{-1})

The thermal initiation behavior (Fig. S45(a-b)) displays that ID_3-2 possesses a ultrafast polymerization phenomenon (200°C for only 10 min) at low concentration compared to the literature [8], revealing its appropriate thermal initiation ability. Additionally, as shown in the solid-state ^{13}C NMR of Fig. S46(a), thermopolymer exhibits two obvious new signals at 170–180 ppm (1) and 42 ppm (2) compared with the HDDA monomer. Signal 1and 2 can be attributed to carbonyl carbon (**C**=O) and its α-position methylene carbon (C=O**C**H_2-), respectively, demonstrating that the bifunctional HDDA initiated by ID_3-2 forms the thermopolymer with network structure. The TG-DSC curves (Fig. S46(b-c)) suggest that the conversion efficiency of thermal polymerization is not as high as that of photopolymerization. However, the thermal polymerization efficiency is appropriate when HDDA is initiated with ID_3-2 at low concentration and heated at a suitable temperature.

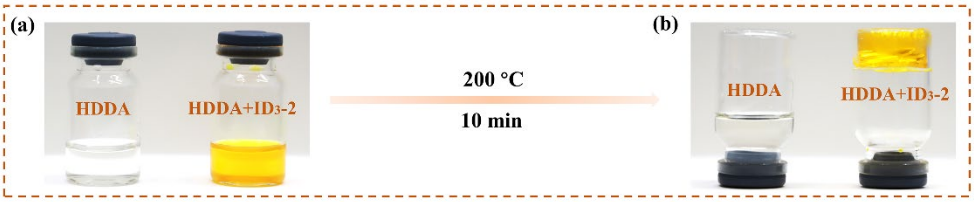

Fig. S45 Deep-layer polymerization of HDDA initiated by ID_3-2 under heating (a) before the heating; after (b) 10 min inverted vial of the heating. (ID_3-2=1×10^{-5} mol g^{-1}, T=200 °C).

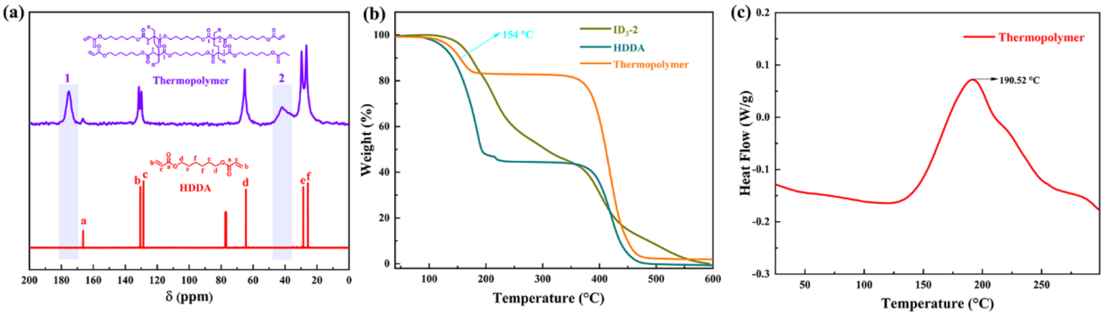

Fig. S46 (a) ^{13}C solid-state NMR spectra of thermopolymer, and liquid ^{13}C NMR of HDDA and ID_3-2 in $CDCl_3$; (b) TG and (c) DSC curve of photopolymer. (Thermopolymer obtained by ID_3-2 initiated HDDA under heating. ID_3-2=1×10^{-5} mol g^{-1}, T=200 °C.)

References

1 Frisch, M. J.; Trucks, G. W.; Schlegel, H. B.; Scuseria, G. E.; Robb, M. A.; Cheeseman, J. R.; Scalmani, G.; Barone, V.; Petersson, G. A.; Nakatsuji, H.; Li, X.; Caricato, M.; Marenich, A. V.; Bloino, J.; Janesko, B. G.; Gomperts, R.; Mennucci, B.; Hratchian, H. P.; Ortiz, J. V.; Izmaylov, A. F.; Sonnenberg, J. L.; Williams-Young, D.; Ding, F.; Lipparini, F.; Egidi, F.; Goings, J.; Peng, B.; Petrone, A.; Henderson, T.; Ranasinghe, D.; Zakrzewski, V. G.; Gao, J.; Rega, N.; Zheng, G.; Liang, W.; Hada, M.; Ehara, M.; Toyota, K.; Fukuda, R.; Hasegawa, J.; Ishida, M.; Nakajima, T.; Honda, Y.; Kitao, O.; Nakai, H.; Vreven, T.; Throssell, K.; Montgomery, J. A.; Peralta, Jr., J. E.; Ogliaro, F.; Bearpark, M. J.; Heyd, J. J.; Brothers, E. N.; Kudin, K. N.; Staroverov, V. N.; Keith, T. A.; Kobayashi, R.; Normand, J.; Raghavachari, K.; Rendell, A. P.; Burant, J. C.; Iyengar, S. S.; Tomasi, J.; Cossi, M.; Millam, J. M.; Klene, M.; Adamo, C.; Cammi, R.; Ochterski, J. W.; Martin, R. L.; Morokuma, K.; Farkas, O.; Foresman, J. B.; Fox, D. J. Gaussian 16, Revision C.01; Gaussian, Inc.: Wallingford, CT, 2016.

2 T. Lu and F. W. Chen, *J. Comput. Chem.*, 2012, **33**, 580-592.

3 C. Xu, S. Gong, X. Wu, Y. W. Wu, Q. Y. Liao, Y. Xiong, *et. al.*, *Dyes Pigments*., 2022, **198**, 110039.

4 R. Liu, H. Chen, Z. Q. Li, F. Shi and X. Y. Liu, *Polym. Chem.,* 2016, **7**, 2457-2463.

5 L. X. Wang, B. Qiu, X. D. An, P. Z. Dong, R. B. Liu, J. Xiao, *Green Chem.,* 2021, **23**, 8181.

6 Z. Q. Li, X. C. Zou, G. G. Zhu, X. Y. Liu and R. Liu, *ACS Appl. Mater. Interfaces.,* 2018, **10**, 16113-16123.

7 C. Jing, G. Ding, X. Z. Qin, G. Y. Peng, H. J. Huang, J. C. Wang, et. al., *Prog. Org. Coat.,* 2017, **110**, 150-161.

8 S. H. Liu, B. Graff, P. Xiao, F. Dumur, and J. Lalevée, *Macromol. Rapid Commun.,*

2021, **42**, 2100207.